Received: 7 February 2018 | Revised: 25 June 2018 | Accepted: 29 June 2018

DOI: 10.1002/hipo.23009

WILEY

RESEARCH ARTICLE

Changes in patterns of neural activity underlie a time-dependent transformation of memory in rats and humans

Melanie J. Sekeres[1,2,3] | Gordon Winocur[1,3,4,5] | Morris Moscovitch[1,3,6] | John A. E. Anderson[1,3,7] | Sara Pishdadian[3,7] | J. Martin Wojtowicz[8] | Marie St-Laurent[1] | Mary Pat McAndrews[3,9] | Cheryl L. Grady[1,3,4]

[1]Rotman Research Institute, Toronto, Ontario, Canada

[2]Department of Psychology and Neuroscience, Department of Biology, Baylor University, Waco, Texas

[3]Department of Psychology, University of Toronto, Toronto, Ontario, Canada

[4]Department of Psychiatry, University of Toronto, Toronto, Ontario, Canada

[5]Department of Psychology, Trent University, Peterborough, Ontario, Canada

[6]Department of Psychology, Baycrest, Toronto, Ontario, Canada

[7]Department of Psychology, York University, Toronto, Ontario, Canada

[8]Department of Physiology, University of Toronto, Toronto, Ontario, Canada

[9]Krembil Research Institute, University Health Network, Toronto, Ontario, Canada

Correspondence
Melanie J. Sekeres, Department of Psychology and Neuroscience, Baylor University, One Bear Place, Waco, TX 76798.
Email: melanie_sekeres@baylor.edu

Funding information
Canadian Institutes of Health Research, Grant/Award Number: MOP125958, MOP14036, Post-Doctoral Fellowship; Natural Sciences and Engineering Research Council of Canada, Grant/Award Number: A8181, Postgraduate Scholarship-Doctoral award; Heart and Stroke Foundation; Canada Research Chairs

Abstract

The dynamic process of memory consolidation involves a reorganization of brain regions that support a memory trace over time, but exactly how the network reorganizes as the memory changes remains unclear. We present novel converging evidence from studies of animals (rats) and humans for the time-dependent reorganization and transformation of different types of memory as measured both by behavior and brain activation. We find that context-specific memories in rats, and naturalistic episodic memories in humans, lose precision over time and activity in the hippocampus decreases. If, however, the retrieved memories retain contextual or perceptual detail, the hippocampus is engaged similarly at recent and remote timepoints. As the interval between the timepoint increases, the medial prefrontal cortex is engaged increasingly during memory retrieval, regardless of the context or the amount of retrieved detail. Moreover, these hippocampal-frontal shifts are accompanied by corresponding changes in a network of cortical structures mediating perceptually-detailed as well as less precise, schematic memories. These findings provide cross-species evidence for the crucial interplay between hippocampus and neocortex that reflects changes in memory representation over time and underlies systems consolidation.

KEYWORDS

context fear conditioning, episodic memory, fMRI, hippocampus, mPFC

1 | INTRODUCTION

Episodic memories in humans can be construed as having two major constituents: (a) central or schematic elements that are critical to the coherence of the event, and (b) perceptual and contextual details that define the event's specificity and impart experiential quality. Episodic memories are vulnerable to progressive loss of perceptual and contextual details (Tulving, 1972), but the schematic elements are retained as more general memories for long periods of time (Brainerd & Reyna, 2002; Winocur & Moscovitch, 2011). Notwithstanding their many differences with human memory, memories in rodents share common features and undergo similar changes. For example, contextual fear memories, when initially formed in rodents, are specific to the contexts in which they were acquired. As with human episodic memories, over time, they become more general and can be evoked in different

environments that retain the general context with few specific details (Wiltgen & Silva, 2007; Winocur, Moscovitch, & Sekeres, 2007).

It is widely accepted that the hippocampus plays an essential role in the initial acquisition and storage of memories in both animals and humans. There is considerable controversy, however, regarding its role in the long-term reorganization of memories. The traditional view holds that the hippocampus's role in memory function is time-limited, after which the same episodic or context-dependent memories become represented in neocortex (Kim & Fanselow, 1992; Squire & Alvarez, 1995; Squire, Genzel, Wixted, & Morris, 2015). A growing body of evidence, however, suggests that cortically-based memories are qualitatively different than the hippocampus-dependent episodic memories (in humans) and context-specific memories (in rodents) (Dudai, 2012; Kandel et al., 2014).

This evidence has given rise to alternative theoretical models that emphasize an enduring role for the hippocampus in mediating human episodic and rodent context-specific memories (Multiple Trace Theory [MTT], Nadel & Moscovitch, 1997), and a transformation process that allows for the representation of schematic or general memories in neocortex (Trace Transformation Theory [TTT], Winocur & Moscovitch, 2011; Sekeres, Moscovitch, & Winocur, 2017). The medial prefrontal cortex (mPFC, Frankland, Bontempi, Talton, Kaczmarek, & Silva, 2004; Takashima et al., 2006; Restivo et al., 2009; Ryan, Roy, Pignatelli, Arons, & Tonegawa, 2015; Bonnici et al., 2012; Bonnici & Maguire, 2017) and other brain regions (posterior cingulate cortex [pCC], precuneus, and angular gyrus, Rugg & Vilberg, 2013) have been implicated in this transformation process.

The present study tests crucial predictions that follow from MTT and TTT; specifically, that reorganized patterns of neural activity, in rats and humans, are related to the quality of a memory as it transforms from one that is perceptually detailed or context-specific to a more schematic or context-general version. The research was also designed to examine several related issues, including the degree of hippocampal activation at remote periods when schematic or generalized memories dominate and, conversely, whether structures, such as mPFC, are implicated in memories that remain context-specific and highly detailed. Notwithstanding differences in tests and delay period, a primary objective of the research was to show that common processes and structures are implicated across species.

In Experiment 1, we tested rats on a contextual fear conditioning task and manipulated context to show that the context-specificity of the learned fear response changes over time. The change in memory expression was accompanied by changes in the pattern of immediate-early gene expression in the hippocampus and mPFC following retrieval. A limitation to current rodent models is the inability to investigate dynamic changes in large-scale neural networks supporting memory across repeated retrieval events. Functional neuroimaging in humans overcomes this limitation. Human episodic memory, like contextual fear memory in rodents, is characterized initially by context-specificity. As in rodents, contextual/perceptual details may be lost over time, while general or schematic features are retained. In Experiment 2, we tested memory for film clips in normal human adults at short and long delays using fMRI to image network activity. We obtained results that complemented those of Experiment 1. This translational approach identifies similarities in hippocampus-dependent memories in rats and humans, and provides evidence for a common memory transformation that can be observed across species.

2 | MATERIALS AND METHODS

2.1 | Experiment 1: The neural basis of context memory transformation in rodents

2.1.1 | Subjects

Male Long-Evans rats (Charles River, QC), three months old at the start of training, served as subjects for the context fear conditioning experiments. Rats were housed in pairs with unlimited access to food and water, and maintained on a 12 hr reversed light cycle (lights off between 0600 and 1800 hr). All behavioral testing occurred during the active phase of the dark cycle. Rats were handled daily for five days prior to training. All procedures were approved by Trent University's Animal Care Committee, and conducted in accordance with the guidelines set by the Canadian Council on Animal Care.

2.1.2 | Apparatus

Context fear conditioning was conducted in a chamber (70 × 31 × 32 cm^3) with horizontal striped black and white side and back walls, and a clear Plexiglas front wall. A speaker was affixed to the left side wall. The chamber floor consisted of metal bars spaced 1.3 cm apart, and the Plexiglas roof was ventilated to allow air circulation. The conditioning chamber was placed on a table, 1.3 m above the floor, located in a sound-attenuated laboratory testing room (2.9 × 1.9 × 2.7 m), dimly lit with overhead lighting. The conditioning chamber served as Context-A (CXT-A) for memory testing. The novel chamber used for Context-B (CXT-B) (29 × 29 × 31 cm^3) had four clear Plexiglas walls, a metal grid floor, and a ventilated Plexiglas roof. The chamber was placed on a desk located in a different sound attenuated test room (4.3 × 3.3 × 2.7 m) with standard laboratory furniture (desk, chairs, sink), and lit by a desk lamp. A video camera was mounted on a tripod in front of each test chamber to record freezing behavior during each condition and test session.

2.1.3 | Behavioral methods

Eight rats were randomly assigned to each of the five conditions: Home cage control, (HC); Short-Delay, CXT-A (SD-A); Short-Delay, CXT-B (SD-B); Long-Delay, CXT-A (LD-A); Long-Delay, CXT-B (LD-B).

2.1.4 | Context pre-exposure and contextual fear conditioning

Prior to fear conditioning, each rat was individually placed in the conditioning chamber and allowed 30 min to explore. The purpose of the context pre-exposure session was to ensure that rats initially formed a robust, context-specific memory for the conditioning context (Winocur et al., 2007). Twenty-four hours later, the rat was transferred back to the test room, placed in the conditioning chamber, and allowed 3 min to explore. Ten tone-shock pairings (tone: 2000 Hz; 90 db, 30 s; shock: 1.5 mA, 1 s) (TechServe, Model 452A shock generator) were then administered with a variable interval (30–120 s)

between pairings. After the last shock, freezing behavior was assessed every 8 s for 64 s (8 observations). The rat was then returned to its home cage.

2.1.5 | Context fear testing

Original Context (CXT-A): Either 24 hr (Short-Delay, SD-A) or 30 days (Long-Delay, LD-A) after conditioning, the rat was returned to the test room, and placed in the conditioning chamber for 8 min. No shock was administered during testing. Freezing behavior was recorded and calculated using an 8-s time sampling procedure for each minute during which freezing was assessed (8 observations per minute, 64 observations total). Freezing behavior was defined as the absence of any visible movement aside from respiration. The percentage of time spent freezing was calculated by dividing the total number of observed freezing responses by eight for each minute. Fear conditioning procedures were adapted from Anagnostaras, Maren, and Fanselow (1999), and have been routinely used in our lab (Winocur et al., 2007; Winocur, Frankland, Sekeres, Fogel, & Moscovitch, 2009; Winocur, Sekeres, Binns, & Moscovitch, 2013). The rat was then returned to its home cage.

Novel-Context (CXT-B): Either 24 hr (Short-Delay, SD-B) or 30 days (Long-Delay, LD-B) after conditioning, the rat was brought to the test room and placed in the novel chamber for 8 min. Testing and scoring of freezing behavior was conducted identically to what is reported for CXT-A. See Figure 1a for a schematic of the study design.

Home Cage (HC) control: The HC group was included to control for baseline expression of the immediate-early gene (IEG) c-Fos. These rats were maintained in their home cages throughout the experiment, and did not undergo any behavioral training or testing. After 30 days, rats were removed from their home cage, sacrificed, perfused, and brains were prepared for immunohistochemistry.

2.1.6 | Perfusion and histology

Immediately following testing, rats were transferred to a quiet, dark holding room. 90 min following test (or HC) conditions, received an overdose IP injection of sodium pentobarbital, and were intracardially perfused using phosphate-buffered saline (PBS) followed by 4% paraformaldehyde (PFA). Brains were removed from the skull, fixed in PFA for 24 hr at 4 °C, then transferred to a PBS and 0.02% sodium azide solution and stored at 4 °C until sectioning. Using a vibratome, brains were sectioned coronally (30 μm slices) across the entire anterior–posterior extent of the brain. Five serial sections per well were stored in a PBS and 0.02% sodium azide solution. For each brain, one section per well was randomly sampled across the range of the anterior cingulate cortex (aCC) and hippocampus. For the aCC, 4–10 sections ranging between 1.70 and −0.92 mm A/P relative to bregma according to the Paxinos and Watson (1997) were sampled for analysis of c-Fos protein expression. For the hippocampus, 10–16 sections ranging between −2.30 mm to −6.04 mm A/P were sampled. 0–3 rats per condition were excluded from c-Fos analysis due to poor tissue integrity resulting in weak immunohistochemical labeling.

2.1.7 | Immunohistochemistry

Coronal brain sections were washed in PBS, then incubated with rabbit anti-c-Fos polyclonal primary antibody (1:1000, PBS and 0.3% Triton X-100, Calbiochem) at 4 °C for 48 hr. Sections were washed 4 × 10 min in PBS, then incubated with donkey-anti-rabbit Alexa 568 secondary antibody (1:200, Molecular Probes) for 2 hr at room temperature. Sections were washed with PBS and then mounted with PermaFluor mounting medium (Thermo Scientific, Fremont, CA) on glass slides, and coverslipped.

2.1.8 | C-Fos quantification

Stained sections were analyzed using a fluorescent microscope (Nikon, MBA 92010 Eclipse NI). Images were taken at 10× magnification using a digital camera (DS-QiMc-U3), and digitally stitched together using NIS-Elements software (Nikon, version 4.1.3) software to reconstruct each region of interest (hippocampus, aCC). Within each section, hippocampal subregions (CA1, CA3, DG) were outlined for the dorsal and ventral regions, then combined to determine dorsal and ventral hippocampal area. c-Fos positive nuclei in each subregion were manually counted using ImageJ (RRID:SCR_003070). For the prefrontal cortical sections, the aCC was outlined, and c-Fos positive nuclei were similarly counted. c-Fos is a commonly used marker of neuronal activity (Greenberg & Ziff, 1983). For each sampled section, c-Fos expression was counted bilaterally for the aCC, and unilaterally for the hippocampus. The total number of c-Fos positive cells per region of interest was divided by the outlined area to generate a normalized cells/area value. c-Fos expression was analyzed for home cage (HC) control brains to determine baseline c-Fos expression in each region of interest. Values of c-Fos positive cells/area from each of the four experimental conditions (SD-A, SD-B, LD-A, LD-B) were divided by the HC control values to determine the percent of change in IEG expression for each condition.

2.1.9 | Experimental design and statistical analysis

A schematic of the experimental timeline can be seen in Figure 1a. ANOVAs were conducted for freezing behavior and on for c-Fos expression measures. All behavioral and histological statistical analyses were conducted using SPSS 23 (RRIS:SCR_002865).

2.2 | Experiment 2: The neural basis of episodic memory transformation in humans

2.2.1 | Participants

Twenty healthy, right-handed participants (12 female), ranging in age from 21 to 31 years old (mean age 24.05, *SD* 2.78), were recruited through the participant database at Baycrest. Participants were fluent in English, and screened using a detailed health questionnaire to exclude psychiatric and neurological disorders, previous head injuries, or other health problems and/or medications that might affect cognitive function and brain activity, including strokes and cardiovascular disease. All procedures were approved by Baycrest's Research Ethics Board, and conducted in accordance with the guidelines set by the Tri-Council Policy Statement: Ethical Conduct for Research Involving Humans. All participants gave written informed consent, and were reimbursed $100 for their participation in the study.

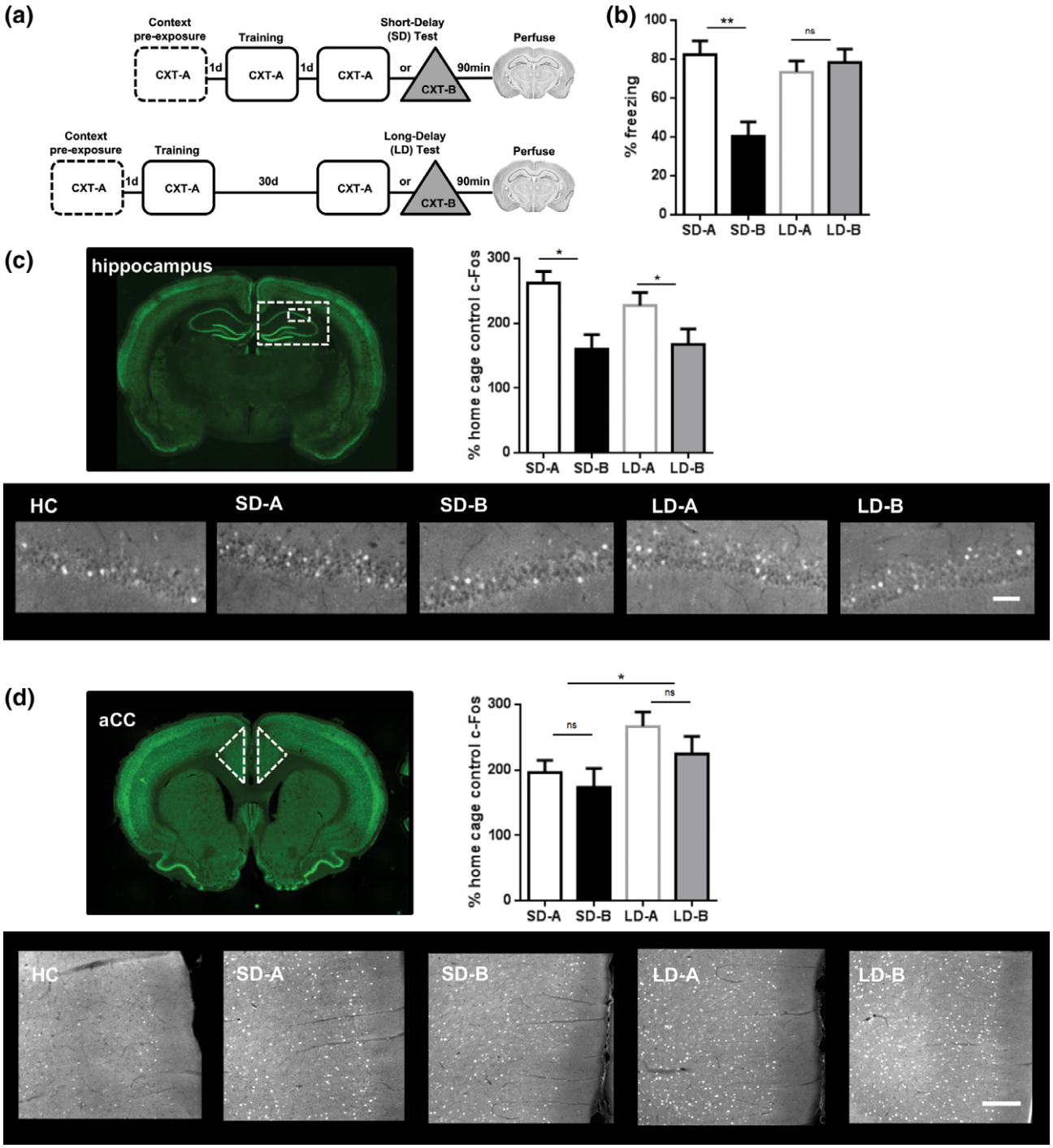

FIGURE 1 The time-dependent generalization of context memory and changes in c-Fos expression. (a) Experimental timeline for the Short-Delay (top) and for the Long-Delay conditions (bottom) in Experiment 1. (b) Mean percent time spent freezing during the first 6 min of the context fear memory test. Rats froze significantly more in CXT-A than in CXT-B at the Short-Delay, but froze at similarly high levels in both CXT-A and CXT-B at the Long-Delay. (c) Left: Coronal sections identifying the hippocampus (outlined in white) stained with NeuN (green) to label all neuronal nuclei. Right: c-Fos expression levels in the hippocampus were significantly higher when tested in CXT-A than in CXT-B. Hippocampal c-Fos expression levels in each context did not differ between the Short and Long-Delay tests. Values are expressed as a percent change from the home cage control baseline c-Fos level. Bottom: Representative c-Fos expression in the hippocampus (CA1 region shown here) for each experimental condition (SD-A, SD-B, LD-A, LD-B) and home cage control (HC) groups. Scale bar = 100 μm (d) Left: Coronal sections identifying the aCC (outlined in white) stained with NeuN (green). Right: c-Fos expression levels in the aCC were significantly higher when tested after a Long-Delay than a Short-Delay. aCC c-Fos expression levels did not differ between the CXT-A and CXT-B test conditions. Vaues are expressed as a percent change from the home cage control baseline c-Fos level. Bottom: Representative c-Fos expression in the aCC for each experimental condition and home cage control groups. Scale bar = 100μm. Error bars represent the *SEM*. * $p < .05$, ** $p < .01$, ^{ns} $p > .05$ [Color figure can be viewed at wileyonlinelibrary.com]

2.2.2 | Behavioral methods

Film clip stimuli

Forty film clips were used to test episodic memory. Film clips have been previously used as naturalistic stimuli for an ecologically-valid memory paradigm (Ben-Yakov & Dudai, 2011; Bird, Keidel, Ing, Horner, & Burgess, 2015; Furman, Dorfman, Hasson, Davachi, & Dudai, 2007; Furman, Mendelsohn, & Dudai, 2012; Sekeres et al., 2016; St-Laurent, Moscovitch, Jadd, & McAndrews, 2014; St-Laurent, Moscovitch, & McAndrews, 2016). Clips were 23 s in duration and were taken from non-English language films with limited dialogue (the same clips were used in previous studies; St-Laurent et al., 2014, 2016; Sekeres et al., 2016; Bonasia et al., 2018). Two series of 20 clips were equated on four feature categories: visual complexity, story complexity, sound complexity, and emotional content to ensure comparable content of clips used at each test delay (Sekeres et al., 2016). For each participant, the two series of clips were pseudo-randomly assigned for testing either immediately (0 d) or 7 d after the encoding session.

2.2.3 | Task

Procedures were based on those developed for a previous study (St-Laurent et al., 2014, 2016). Prior to scanning, participants were read a set of instructions, and then performed a practice session in which they watched two sample clips and performed the memory retrieval task. Participants were told they would be tested on their memory for the clips following varying delays, and instructed not to rehearse the information in the interim. Once in the scanner, they were again briefed on the instructions for the task. All experimental stimuli were viewed through a mirror affixed to the head coil, and responses to the memory ratings were recorded using a button box taped to the right hand. Experimental stimuli were presented using E-Prime 2 (version 2.0.10.242, E-Studio, Psychology Software Tools Inc.).

2.2.4 | Encoding session in scanner

During encoding, participants viewed the 40 film clips, presented in randomized order. Each clip was given a unique title (i.e., "Boy, Girl and Balloon") that served as a retrieval cue in the retrieval portion of the experiment. The title appeared centrally on the screen for 4 s immediately before and after the clip played. Clips were centrally presented on a computer screen. Sound was delivered through a rimless Avotech headset. Participants were instructed to pay attention to the title and content of each clip. A fixation cross was presented for 4 s between each clip. Encoding occurred across four runs in the scanner, with 10 clips presented in each run. No response was required during the encoding session. Immediately after the four encoding runs, a 5 min resting state scan was conducted. See Figure 2a,b for study timeline and design schematics.

2.2.5 | Retrieval session in scanner

Memory for a series of 20 clips (see Film Clip Stimuli) was tested either immediately (0 d) after the encoding session, or after a 7 days delay (7 d). Clips were assigned pseudo-randomly to a retrieval session timepoint in a manner that was counterbalanced across participants. Participants were presented with the title of a clip for 16 s, during which they were instructed to visualize the clip in their mind, from beginning to end. Next, they used a key pad to rate their memory retrieval for the clip's story content, on a scale of 1 (no story content) to 4 (all story content). Story content refers to the central plot line of the story (what happened), and events central to the progression of the episode (Berntsen, 2002; Sekeres et al., 2016; St-Laurent et al., 2014, 2016). Next, participants rated the vividness of perceptual details retrieved in a similar way (rating of 1 = no perceptual details, rating of 4 = most vivid memory). Perceptual details referred to visual (colors, lighting, textures, facial features, clothing, positions of objects, background details, weather, lighting conditions, etc.) and auditory details (talking, laughing, background music, street sounds). A fixation cross presented centrally on the screen for 4 s separated the retrieval period for each clip.

2.2.6 | Retrieval session outside scanner

Participants next performed a postscan test session. During this session, participants were again cued with the title of the clip they had retrieved in the scanner, and asked to verbally report the story content details they recalled while in the scanner (what happened, who did what, what was the situation). Participants were next asked to verbally report, within a maximum of 60 s, any perceptual (visual or auditory) details they experienced in their mind's eye while they recalled the clip in the scanner. Recordings of verbal responses were transcribed and scored according to a system described below. The presentation order of clips was randomized within each retrieval session. The postscanning retrieval testing was conducted on a desktop computer using E-Prime 2 in a sound-attenuated room. Recording failed during the verbal retrieval session for one participant, so verbal retrieval data are presented for 19 participants.

2.2.7 | Scoring and analysis of behavioral data

Self-report ratings of story content and vividness of perceptual details were averaged across clips for each delay. As described above, two separate recordings of the verbal retrieval responses were obtained for each clip to encourage participants to report what they recalled about a clip's storyline and perceptual content. The recordings were manually transcribed and responses were coded and scored to categorize central elements (indicative of story content) and peripheral details (reflecting perceptual details). Central elements were story details that could not be modified or omitted without changing the plotline of the story (Berntsen, 2002). To score central elements consistently, 5 to 6 central story points were identified for each clip and recorded as a "central narrative" (see Sekeres et al., 2016 for a list of central story points for each clip, and for an example of a coded transcript). A participant was given a score of one for each item of retrieved information that corresponded to a point in the central narrative for that clip. Peripheral details were considered any additional descriptive information, including perceptual, and emotional details. One peripheral point was scored for each peripheral story detail reported during the verbal retrieval session. Notably, there was an upper limit to the number of central points a participant could score, but no such limit for peripheral points. To control for the different baseline conditions for each type of detail (central or peripheral), a *t* test (two-tailed) of the percentage of details retained (i.e., Percent

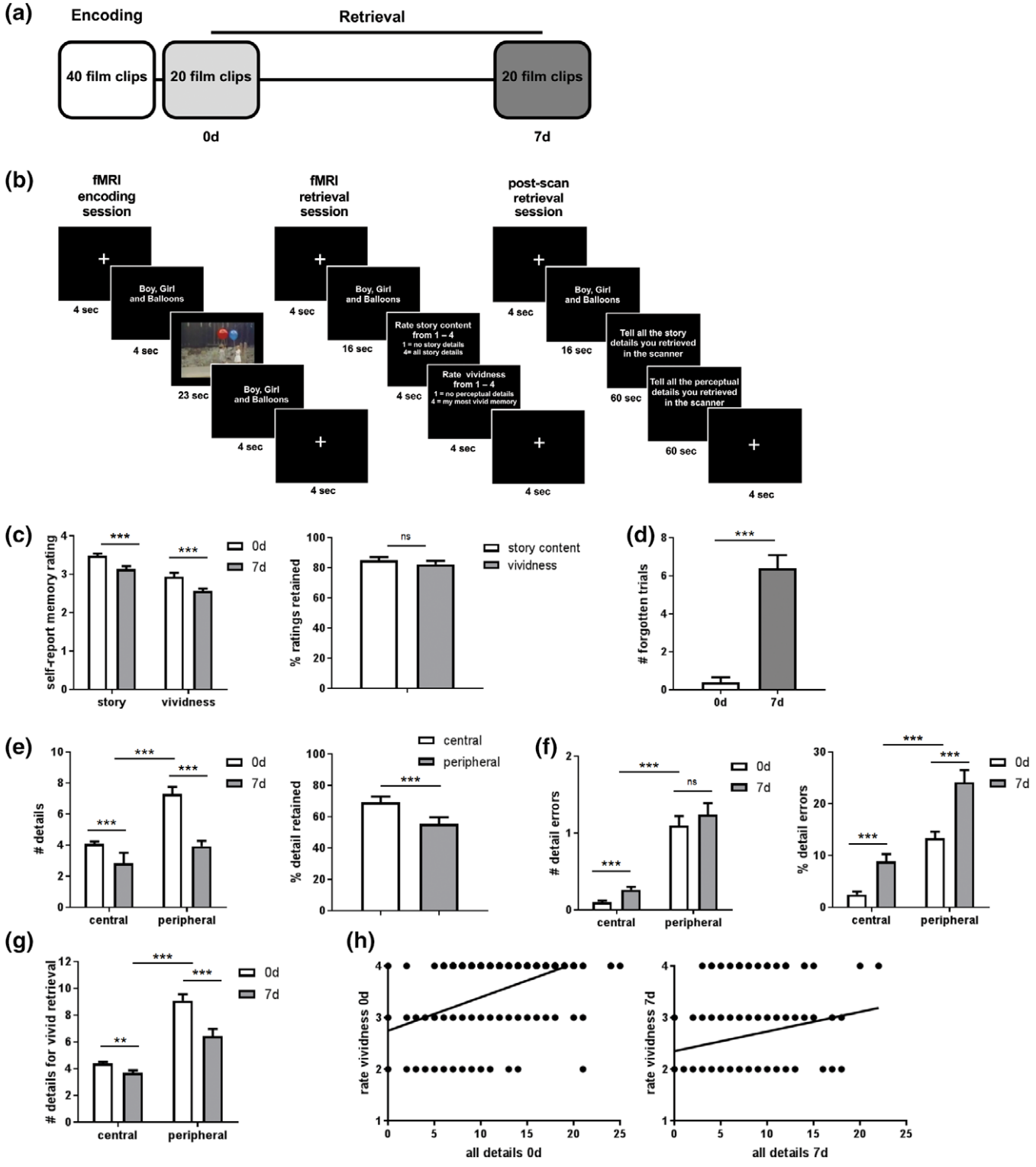

FIGURE 2 Time-dependent schematization of episodic memory. (a) Experimental timeline for Experiment 2. (b) Detailed schematic of the study design for the encoding session (left), in-scan retrieval session (middle), and postscan retrieval session (right). Encoding session: 40 film clips were shown to participants in a randomized order. Retrieval session: The retrieval sessions were identically run across each delay (0 and 7 days). (c) Left: In-scanner memory ratings of the story content and the vividness of perceptual details for each memory retrieval test session (0 day delay, white bars; 7 days delay, gray bars). Participants rated their memory for the story content more highly than the vividness of their memory for the perceptual details in the film clips. Right: Percent of memory ratings retained between the 0 and 7 days in-scanner retrieval sessions. The memory ratings declined at similar levels for both story content and vividness of perceptual details over the course of 1 week. (d) Mean number of forgotten trials at the 0 and 7 days delay. Forgotten trials were classified based on in-scanner memory ratings of 1 (lowest rating) for both story content and perceptual content. (e) Left: Number of details (central elements and peripheral details) reported during the postscanner verbal memory retrieval test session at each delay. Participants reported more peripheral details than central elements when tested immediately (white bars) after encoding but similar levels of central elements and peripheral details when tested 7 days (gray bars) following encoding. Right: Percent

Retained = [(7 d/0 d) × 100]) between the immediate retrieval (0 d) test and the 7 d retrieval test was also conducted.

For each clip, both central elements and peripheral details were coded and tallied across the first recording (participant probed for story content) and second recording (participant probed for perceptual details) by an experimenter (S.P.) blind to the delay condition. A subset of recordings was scored by a second experimenter (M.J.S.) to confirm an acceptable rate of 90% inter-rater reliability in detail scoring. Each reported detail was classified as either central or peripheral. No additional points were assigned for repeated details, or for unrelated information about the film clips (i.e., opinions or speculations). Errors in central elements and peripheral details were also calculated. Errors were considered to be any recalled details that did not match the information presented in the film clip. For each type of detail (central or peripheral), the total number of errors was subtracted from the total number of correct details for each clip (i.e., Retrieval Success = # correct details – # errors) to determine the corrected memory retrieval success scores used in the final data analyses. For each participant, the corrected central and peripheral details were averaged across all clips for each delay condition (0 and 7 days). We also assessed the percentage of errors as a proportion of all reported central and peripheral details.

For all behavioral analyses, we excluded "forgotten" retrieval trials, which were trials given memory retrieval ratings of "1" (indicating low memory for story content and low vividness of perceptual details), and for which there were no central elements or peripheral details reported during the verbal retrieval session. We also excluded trials in which the participant reported details corresponding to the wrong film clip (never more than one clip per participant). Although these data were excluded in the main analyses, analyses that included these data produced the same pattern of results (data not shown, but available on request).

3 | EXPERIMENTAL DESIGN AND STATISTICAL ANALYSIS

A schematic of the experimental timeline and design can be seen in Figure 2a,b. Repeated measures ANOVAs were conducted for the ratings, detailed retrieval, and error measures, and *t* tests were conducted to assess differences in the percentage of rating and details retained, and for differences the number of forgotten trials between 0 and 7 days retrieval. Data analysis was performed using SPSS 23. Statistical analyses of brain imaging data are described below.

3.1 | fMRI methods

3.1.1 | Image acquisition and preprocessing

Participants were scanned using a Siemens Trio 3 T scanner. Anatomical scans were acquired with a three-dimensional magnetization-prepared rapid acquisition with gradient echo (MP-RAGE) sequence (repetition time (TR) = 2000 ms, echo time (TE) = 2.6 ms, field of view (FOV) = 256 mm, slice thickness = 1 mm, 160 slices. Functional runs were acquired with an echo planar imaging (EPI) sequence, with 139 volumes for each retrieval run (TR = 2.2 s, TE = 27 ms, flip angle = 62°, FOV = 225 mm, 64 × 64 matrix, 36 3.5 mm (skip 0.5 mm) thick axial slices, positioned to image the whole brain. Slices were obtained from an axial oblique orientation, parallel to the Sylvian fissure.

Preprocessing of the image data was performed with Analysis of Functional Neuroimages (AFNI, Cox, 1996). This processing included regressing out physiological artifact using RETROICOR, rigid motion correction, spatial normalization to Montreal Neurological Institute (MNI) space, and smoothing with an 8 mm Gaussian filter (the final voxel size was 4 × 4 × 4 mm). We also regressed out white matter, cerebral spinal fluid, and vasculature (Anderson, Campbell, Amer, Grady, & Hasher, 2014; Campbell, Grigg, Saverino, Churchill, & Grady, 2013). As motion has been demonstrated to affect brain-activity measures, even after standard correction procedures (Power, Barnes, Snyder, Schlaggar, & Petersen, 2012), we followed a motion-scrubbing procedure described in Campbell et al., 2013. Briefly, this procedure uses a multivariate technique to identify outliers in both the motion-parameter estimates and fMRI signal itself. Where such outliers co-occurred (never more than 5% of the total volumes), we removed the fMRI volumes and replaced them with values interpolated with cubic splines. This method has the advantage of suppressing spikes, yet keeping the length of the time course intact across subjects.

3.1.2 | Partial-least-squares analysis

The image data were analyzed with Partial Least Squares (PLS; McIntosh, Bookstein, Haxby, & Grady, 1996; McIntosh & Lobaugh, 2004), a multivariate analysis technique that identifies whole-brain patterns of covariance related to the experimental design (task PLS) in a single step for multiple groups. This method is similar to principal component analysis (PCA), in that it identifies a set of principal components, or "latent variables" (LVs), which optimally capture the covariance between two sets of measurements (Friston, Frith, Liddle, & Frackowiak, 1993). PLS uses singular value decomposition in

of memory details retained between the 0 and 7 days postscanner retrieval sessions. Over the course of 1 week, peripheral details were forgotten at a higher rate than central elements. (f) Left: Mean number of errors per trial during the 0 day (white bars) and 7 days (gray bars) postscan verbal retrieval. Errors were subtracted from the total number of retrieved details to produce the corrected number of central and peripheral details at each delay (Retrieval Success). Right: Mean percentage of errors as a proportion of the total number of correctly reported details per trial during the 0 and 7 days postscan verbal retrieval. (g) Number of details (central elements and peripheral details) reported during the postscanner verbal memory retrieval test session for those clips classified as having been retrieved with high vividness (receiving in-scanner ratings of 3.4) at each delay. Participants reported more peripheral details than central elements at both 0 day (white bars) and 7 days (gray bars) retrieval sessions. (h) Plot of the total number of details (all details = central + peripheral details) recalled and vividness rating for 0 day (left), and 7 days delayed retrieval (right). Each plot includes the best fitting linear regression line. Error bars represent the *SEM*. $*p < .05$, $**p < .01$, $***p < .001$, $^{ns}p > .05$ [Color figure can be viewed at wileyonlinelibrary.com]

a data-driven approach to reduce the complexity of the data set into orthogonal LVs that attempt to explain the maximum amount of covariance between the task conditions and the BOLD signal. In task PLS, each brain voxel has a weight, known as a salience, indicating how strongly that voxel contributes to the LV overall. The significance of each LV as a whole was determined with a permutation test (McIntosh et al., 1996) using 1,000 permutations. In addition, the reliability of each voxel's contribution to a particular LV was tested by submitting all saliences to a bootstrap estimation of the standard errors (*SE*s; Efron, 1981), using 1,000 bootstraps. Peak voxels with a salience/*SE* ratio ≥ 3.0 ($p < .001$) are considered to be reliable (Sampson, Streissguth, Barr, & Bookstein, 1989).

Clusters containing at least five reliable contiguous voxels were extracted, with a local maximum defined as the voxel with a salience/*SE* ratio higher than any other voxel in a 2 cm cube centered on that voxel (the minimum distance between peaks was 5 mm). Coordinates of these locations are reported in MNI standard coordinate space (Mazziotta et al., 2001). Because the extraction of the LVs and the corresponding brain images is done in a single step, no correction for multiple comparisons is required. Finally, to obtain summary measures of each participant's expression of each LV spatial pattern, we calculated brain scores by multiplying each voxel's salience by the BOLD signal in the voxel, and summing over all brain voxels for each participant in each condition. These brain scores were then mean-centered (using the grand mean across all subjects and conditions) and confidence intervals (CIs; 95%) for the mean brain scores in each condition were calculated from the bootstrap. Following procedures used elsewhere (Anderson et al., 2014; Garrett, Kovacevic, McIntosh, & Grady, 2010; Grady et al., 2010; McIntosh, Chau, & Protzner, 2004), conservative estimates of differences in activity between conditions and between groups were determined by a lack of overlap in these bootstrapped CIs. That is, nonoverlapping intervals between conditions within a group, or between groups within a condition, indicated a significant difference.

3.1.3 | fMRI task analysis

To assess modulations of BOLD activity across the conditions, we first conducted a mean-centered task PLS analysis (blocked design, where each clip was defined as a block) that contrasted the mean activity (averaged over all blocks across runs) in the retrieval task and fixation at the immediate (0 d) and 7 days delay conditions (Figure 3a,c, Table 1). Brain scores associated with each LV are shown in Figure 3b, d. We also ran a PLS analysis directly contrasting the 0 and 7 days retrieval tasks (Figure 3e,f, Table 2). All retrieval analyses contained trials in which participants reported successfully retrieving the story and perceptual content from the clip (ratings of 2, 3, or 4). Forgotten trials (assigned in-scanner ratings of 1 s) were excluded from the retrieval analyses. Finally, we contrasted clips that were recalled with high vividness (in-scanner ratings of 3 and 4 for both story content and perceptual details; Geib, Stanley, Wing, Laurienti, & Cabeza, 2015) between the 0 and 7 days retrieval tasks to determine differences in retrieval activity at each delay when the memory for the clips remained vivid (Figures 2g,h and 4a,b, Table 3). The number of vividly retrieved clips at each delay ranged from 7 to 19 clips for 0 day delay and 1 to 14 clips for 7 days delay. We performed Pearson's correlations to assess the relationship between participant's subjective ratings of retrieval and the quality of the retrieved memories for individual clips included in the retrieval activity analyses at 0 and 7 days (Figure 2h). We also ran analyses for the highly vivid trials including only participants with at least 5 ($n = 16$), at least 6 ($n = 13$), and at least 7 ($n = 10$) of the highly vivid trials, and obtained similar results as the analysis that included all subjects (data not shown, but available on request).

4 | RESULTS AND COMMENT

4.1 | Experiment 1: The neural basis of context memory transformation in rodents

4.1.1 | Behavioral results: Retrieval of contextual fear memory

We first set out to replicate our previous behavioral findings to demonstrate the reliability of contextual fear generalization over time (Einarsson, Pors, & Nader, 2014; Wiltgen & Silva, 2007; Winocur et al., 2007). Freezing behavior, the measure of fear memory, was assessed in the original conditioning context (CXT-A), or in a novel context (CXT-B) following a short delay (SD; 1 day) or a long delay (LD; 30 days). The time course of freezing was assessed over an 8 min test period for each of the four groups. As all groups showed a decline in freezing in the last 2 min of the test, only the first 6 min of the test were analyzed (8 min test data not shown, but available on request). A 2 × 2 ANOVA assessed freezing behavior, with Context (CXT-A, CXT-B) and Delay (SD, LD) as between-subject factors. Significant main effects were found for Context, with more freezing in CXT-A than in CXT-B ($F_{[1,31]} = 7.178$, $p = .012$, $\eta_p^2 = 0.204$), and for Delay, with more freezing at the LD than SD ($F_{[1,31]} = 4.409$, $p = .045$, $\eta_p^2 = 0.136$). A significant Context x Delay interaction ($F_{[1,31]} = 11.184$, $p = .002$, $\eta_p^2 = 0.285$) confirmed that rats exhibited context-specific memory at the short delay, freezing at higher levels in CXT-A than CXT-B ($t_{[14]} = 3.977$, $p = .001$). At the long delay, groups displayed equivalent levels of freezing in both contexts ($t_{[14]} = -0.509$, $p = .619$) (Figure 1b), consistent with the idea that the memory generalized over time. These effects mirror those observed in a previous study using these same parameters (Winocur et al., 2007), and provide validation for the next stage of the research which aimed to identify underlying patterns of neural activity supporting changes in the quality of context memory over time.

4.1.2 | C-Fos results: Analysis of c-Fos expression

To test the prediction that the retrieval of generalized memory is increasingly supported by medial prefrontal cortical regions, while retrieval of the context-specific memory engages the hippocampus, we analyzed expression of c-Fos using immunohistochemistry in the hippocampus and the aCC (Figure 1c,d). To assess c-Fos expression in the hippocampus, a 2 × 2 ANOVA was conducted with Context and Delay as between-subject factors. A significant main effect was found for Context, with higher c-Fos expression following context memory

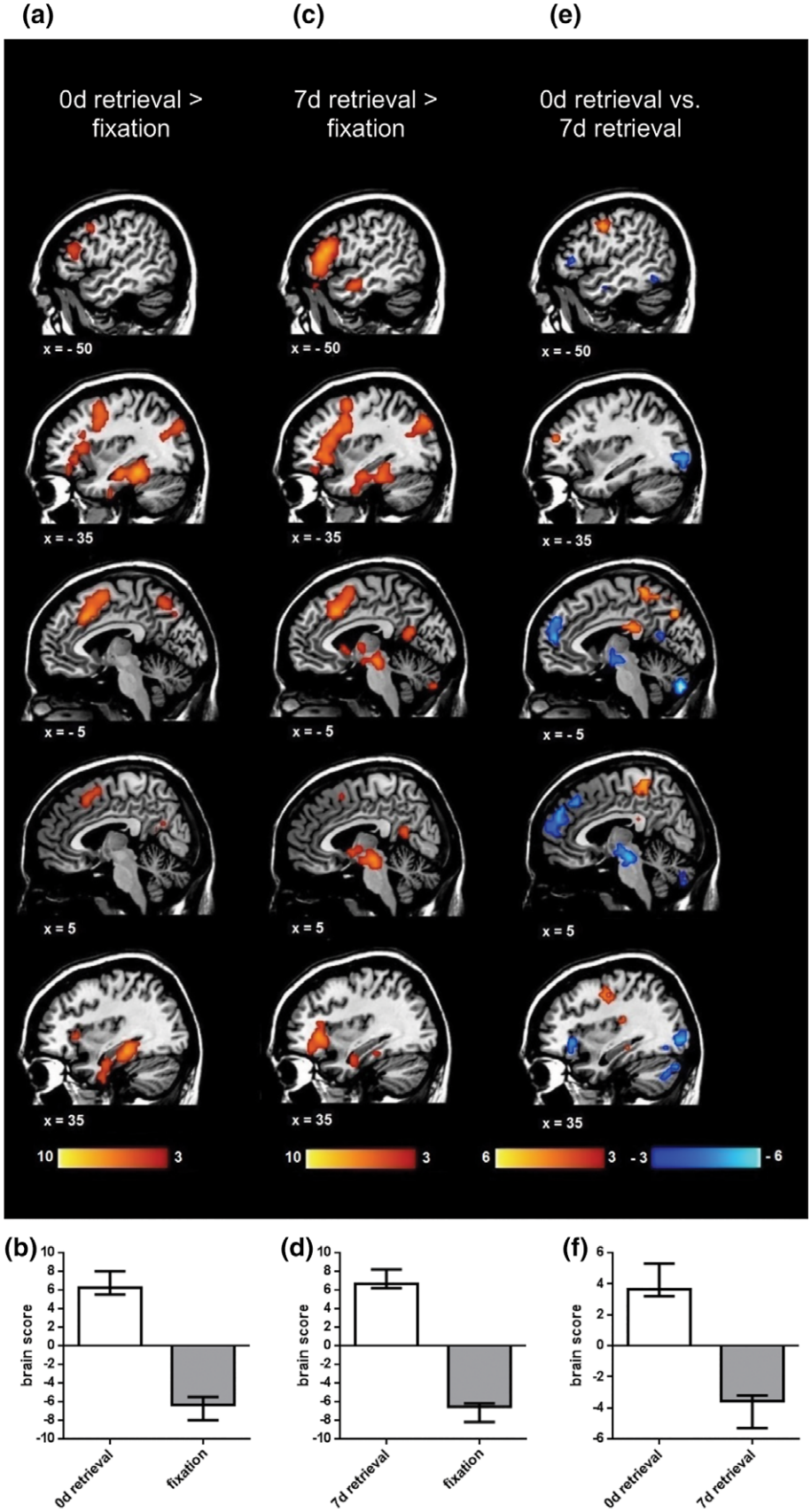

FIGURE 3 Time-dependent changes in the network of brain regions active during memory retrieval. Mean-centered, blocked design PLS analyses were conducted to assess modulations in BOLD activity across the brain during memory retrieval. (a) LV depicting brain activity associated with immediate (0 day) retrieval (warm colors) contrasted with fixation (areas with more activity during fixation are not shown on figure). Note the anterior and posterior hippocampal activation during the immediate retrieval task. (b) Brain scores reflecting the degree to which 0 day retrieval (positive BSRs) and fixation (negative BSRs) correlate with the pattern of activity seen in (a). (c) LV depicting brain activity associated with 7 days

testing in CXT-A than in CXT-B ($F_{[1,23]}$ = 10.758, p = .004, η_p^2 = 0.350), but a nonsignificant main effect of Delay ($F_{[1,23]}$ = 0.327, p = .574, η_p^2 = 0.016) and a nonsignificant Context x Delay interaction ($F_{[1,23]}$ = 0.727 p = .404, η_p^2 = 0.035; Figure 1c). A similar pattern of results was found in both the dorsal and ventral hippocampus (data not shown, but available on request). Post hoc t tests confirmed higher hippocampal c-Fos expression in rats tested in CXT-A at the short delay ($t_{[9]}$ = 2.938, p = .017) and at the long delay ($t_{[13]}$ = 2.426, p = .029).

To assess c-Fos expression in the aCC, a 2 × 2 ANOVA was conducted with Context and Delay as between-subject factors. A significant main effect was found for Delay, with higher c-Fos expression at memory retrieval in the LD condition ($F_{[1,28]}$ = 5.789, p = .024, η_p^2 = 0.188), but a nonsignificant main effect of Context ($F_{[1,28]}$ = 1.654, p = .210, η_p^2 = 0.062) and no significant Context × Delay interaction ($F_{[1,28]}$ = 0.146 p = .705, η_p^2 = 0.006, Figure 1d).

Together, these results support the time-dependent shift in retrieval-associated activity within the hippocampus and mPFC nodes of the context fear memory network. The hippocampus is sensitive to context-specificity at both short and long delays, whereas it is primarily the prefrontal cortex that mediates the time-dependent generalization of the memory across contexts. Contrary to the traditional view of consolidation, these results suggest that the memory supported by the prefrontal cortex at long delays is qualitatively different (more generalized) from the memory that strongly engages the hippocampus. These results also suggest that although the hippocampus continues to be recruited for context-specific remote memory retrieval, a reorganized memory trace forms in the medial prefrontal cortex over time, and it is the latter that dominates behavioural performance at remote intervals.

4.2 | Experiment 2: The neural basis of episodic memory transformation in humans

4.2.1 | Behavioral results

In-scanner retrieval

Memory for short film clips was tested during fMRI scanning either immediately following encoding (0 day), or after a delay of 1 week (7 days). Significantly more film clips were forgotten during the 7 days retrieval session compared to immediate (0 day) retrieval ($t_{[19]}$ = −8.718, p < .0001) (Figure 2d), with a range of 0–5 forgotten clips during 0 day retrieval, and a range of 1–11 forgotten clips during 7 days retrieval.

A 2 × 2 repeated measures ANOVA was conducted with Rating Type (story content and vividness) and delay (0 and 7 days) as within-subject factors, and the assigned ratings as the dependent variable. The ANOVA revealed significant main effects of Rating Type ($F_{[1,19]}$ = 73.908, p < .0001, η_p^2 = 0.795), with participants giving higher ratings for story content over vividness, and of Delay ($F_{[1,19]}$ = 55.555, p < .0001, η_p^2 = 0.745), with a decrease in memory ratings over time. There was no significant interaction between Rating Type x Delay ($F_{[1,19]}$ = 0.209, p = .653, η_p^2 = 0.001; Figure 2c, left). This was confirmed by a paired-samples t test for the percentage of ratings retained over time. The t test revealed no significant difference between the percentage of story content or perceptual vividness ratings between the immediate and 7 days retrieval sessions ($t_{[19]}$ = 1.167, p = .257; Figure 2c, right). Together, these results suggest that participants judged that their memory declined equally over time for both main story content as well as the accompanying perceptual detail.

Postscan retrieval

The qualitative content of the memories was evaluated immediately following each scanning session. Consistent with our previous work (Sekeres et al., 2016), participants demonstrated a greater loss of peripheral details (indicative of perceptual information) than of central elements (reflecting the schematic story content) over time. A 2 × 2 repeated measures ANOVA was conducted with Detail Type (central and peripheral) and Delay (0 and 7 days) as within-subject factors, and the number of correctly recalled details (Retrieval Success) as the dependent variable. The ANOVA revealed significant main effects of Detail Type ($F_{[1,18]}$ = 57.977, p < .0001, η_p^2 = 0.763), with more peripheral details recalled than central elements, and of Delay ($F_{[1,18]}$ = 75.844, p < .0001, η_p^2 = 0.808), indicating that participants recalled fewer details after 7 days. A significant Detail Type × Delay interaction ($F_{[1,18]}$ = 48.723, p < .0001, η_p^2 = 0.730) showed that, although memory for both detail types declines over time, memory for peripheral details suffered a significantly greater decline than memory for central elements (Figure 2e, left). Given that participants recalled central elements near ceiling levels during 0 day retrieval, we next confirmed that the differential rates of forgetting were not due to the different maximal number of retrievable peripheral details and central elements by conducting an additional analysis using percentage of details retained as the dependent variable. Consistent with the previous result, this analysis revealed a significantly greater percentage of retained central elements than of peripheral details over a week's delay ($t_{[18]}$ = 4.735, p < .001; Figure 2e, right). These results indicate that memory for peripheral details declined disproportionally over the week following encoding, whereas memory for central story elements was preferentially retained. Of interest, this pattern was not reflected in subjects' vividness ratings, as they reported equivalent retention of both story (central) and perceptual (peripheral) content.

delayed retrieval (warm colors) contrasted with fixation (data not shown on figure). Note the less extensive posterior hippocampal activation, and the increased medial prefrontal activation during the 7 days retrieval task. (d) Brain scores reflecting the degree to which 7 days retrieval (positive BSRs) and fixation (negative BSRs) correlate with the pattern of activity in (c). (e) LV depicting brain activity associated with immediate (0 day) retrieval (warm colors) contrasted with 7 days delayed retrieval (cool colors). (f) Brain scores reflecting the degree to which 0 day retrieval (positive BSRs) and the 7 days retrieval (negative BSRs) correlate with the pattern of activity in (e). Error bars are 95% confidence intervals. fMRI results are displayed using Mango (Research Imaging Institute, UTHSCSA). PLS = Partial Least Squares; BOLD = blood-oxygen-level dependent; LV = latent variable; BSR = bootstrap ratio [Color figure can be viewed at wileyonlinelibrary.com]

TABLE 1 Coordinates of regions associated with memory retrieval

Hem	Brain region	BA	*X* (mm)	*Y* (mm)	*Z* (mm)	BSR	Cluster size (voxels)
0 day retrieval > fixation							
Left	Inferior frontal gyrus	45	−40	20	8	4.53	69
Left	Inferior frontal gyrus[a]	47	−32	32	−8	4.68	31
Right	Precentral gyrus	44	40	4	32	4.22	5
Left	Middle cingulate cortex	24	−4	24	36	7.68	315
Right	Middle temporal gyrus	21	52	4	−24	4.15	10
Right	Middle temporal gyrus	39	40	−52	16	4.97	19
Left	Inferior temporal gyrus	20	−36	−8	−40	3.9	9
Right	ParaHippocampal gyrus[a]	37	36	−32	−16	8.39	86
Left	Fusiform gyrus[a]	37	−28	−36	−20	9.55	190
Right	Precuneus[a]	30	24	−56	20	10.1	93
Left	Precuneus[a]	7	−12	−60	48	5.21	59
Right	Insula lobe	47	32	24	0	4.16	8
Left	Middle occipital gyrus	39	−36	−68	20	4.71	39
Left	Calcarine gyrus	17	−16	−60	16	4.96	43
Left	Putamen		−20	16	4	4.73	41
Right	Caudate nucleus		20	16	12	5.31	37
7 days retrieval > fixation							
Right	Superior frontal gyrus	8	20	24	52	4.01	13
Right	Superior frontal gyrus	9	20	48	28	4.91	5
Right	Middle frontal gyrus	46	32	32	36	5.79	9
Right	Middle frontal gyrus	45	44	48	8	3.6	5
Left	Middle frontal gyrus	6	−36	4	52	5.53	8
Left	Middle frontal gyrus	9	−32	28	40	3.92	15
Left	Middle frontal gyrus	45	−44	44	16	4.92	10
Right	Inferior frontal gyrus	46	44	20	20	3.76	8
Left	Inferior frontal gyrus	46	−48	24	16	8.64	78
Left	Inferior frontal gyrus[a]	47	−28	28	−4	10.81	593
Right	Insula lobe	47	32	24	−4	6.85	76
Left	Superior medial gyrus	0	−4	20	40	7.61	97
Right	Middle temporal gyrus	21	52	0	−24	6.56	62
Left	Middle temporal gyrus[a]	20	−52	−8	−20	4.87	24
Right	Hippocampus[a]		20	−12	−20	4.5	9
Right	Fusiform gyrus[a]	37	40	−40	−20	3.24	10
Left	Fusiform gyrus[a]	20	−36	−32	−28	5.01	107
Right	Precuneus[a]	17	24	−56	20	7.46	117
Right	Middle occipital gyrus	39	48	−68	24	3.58	7
Left	Middle occipital gyrus	19	−36	−80	36	6.14	51
Right	Putamen		20	12	0	5.38	61
Right	Cerebellum		12	−76	−36	5.04	26
Left	Cerebellum		−8	−80	−40	4.48	10

Note. Top: MNI coordinates of the peak activation voxel within each cluster are reported for the contrast of immediate (0 day) retrieval to fixation (warm color activations in Figure 3a, positive BSRs, data for fixation > retrieval are not shown in Figure 3a). Bottom: MNI coordinates of the peak activation voxel within each cluster are reported for the comparison of 7 days retrieval to fixation (warm color activations in Figure 3c, positive BSRs, data for fixation > retrieval are not shown in Figure 3c). Hem = hemisphere; BA = Brodmann Area; BSR = bootstrap ratio from the PLS analysis indicating the robust contribution of the reported voxel.

[a] Indicates the cluster contains structures within the retrieval network.

To assess changes in errors during memory retrieval, a 2 × 2 repeated measures ANOVA was conducted with Detail Type (central and peripheral) and Delay (0 and 7 days) as within-subject factors. The ANOVA revealed significant main effects of Detail Type ($F_{[1,18]}$ = 81.133, p < .0001, η_p^2 = 0.818) with more errors in peripheral details than central elements, and of Delay ($F_{[1,18]}$ = 4.724, p = .043, η_p^2 = 0.208), indicating that participants made more errors during the 7 days retrieval session. There was no significant Detail Type × Delay interaction ($F_{[1,18]}$ = 0.036, p = .852, η_p^2 = 0.002; Figure 2f). We also assessed the percentage of reported errors as a proportion of the total number of reported details. The ANOVA revealed significant main effects of Detail Type ($F_{[1,18]}$ = 85.773, p < .0001, η_p^2 = 0.870) with a

TABLE 2 Coordinates of regions associated with immediate and 7 days delayed retrieval

Hem	Brain region	BA	*X* (mm)	*Y* (mm)	*Z* (mm)	BSR	Cluster size (voxels)
0 day retrieval > 7 days retrieval							
Left	Middle frontal gyrus	45	−40	48	20	3.98	9
Right	Precentral gyrus	6	56	0	44	4.14	37
Right	Precentral gyrus	6	20	−24	64	3.57	7
Left	Precentral gyrus	6	−48	−4	40	4.06	19
Right	Rolandic operculum	48	40	−28	20	3.62	5
Left	Paracentral lobule	6	−12	−12	68	3.72	6
Left	Paracentral lobule	4	−16	−32	64	3.71	7
Right	Hippocampus[a]		40	−32	−12	4.84	5
Right	Superior parietal lobule	7	20	−72	48	5.22	59
Left	Precuneus[a]	7	−8	−76	40	4.96	55
Left	Precuneus[a]	7	0	−40	52	4.05	55
0 day retrieval < 7 days retrieval							
Right	Superior medial frontal gyrus	32	8	32	40	−4.63	16
Left	Superior medial frontal gyrus[a]	9	0	52	32	−5.13	88
Right	Inferior frontal gyrus	48	40	24	24	−3.72	12
Right	Inferior frontal gyrus	45	56	36	0	−3.84	5
Right	Inferior frontal gyrus[a]	47	32	24	−8	−4.02	23
Left	Inferior frontal gyrus[a]	11	−24	32	−8	−4.38	14
Left	Inferior frontal gyrus	45	−52	32	0	−3.35	5
Right	Middle temporal gyrus[a]	20	52	−4	−28	−5.08	5
Left	Inferior temporal gyrus[a]	21	−56	−4	−28	−4.01	6
Left	Precuneus[a]	31	−4	−60	16	−3.73	6
Left	Caudate nucleus	25	−8	12	8	−3.72	4
Left	Putamen	48	−16	4	−8	−3.93	5
Right	Middle occipital gyrus	18	36	−92	0	−4.62	29
Left	Inferior occipital gyrus	18	−32	−92	−8	−4.49	39
Right	Cerebellum		12	−76	−36	−5.09	42
Right	Cerebellum	19	28	−76	−20	−3.72	9
Right	Cerebellum		36	−84	−32	−4.36	7
Left	Cerebellum		−4	−80	−40	−6.76	24

Note. MNI coordinates of the peak activation voxel within each cluster are reported for LV1 for the PLS analysis of 0 day retrieval (warm color activations in Figure 3e, positive BSRs) contrasted with 7 days retrieval (cool color activations in Figure 3e, negative BSRs). Hem = hemisphere; BA = Brodmann Area; BSR = bootstrap ratio from the PLS analysis indicating the reliability of the reported voxel.
[a] Indicates the cluster contains structures within the retrieval network.

greater percentage of peripheral detail errors than central detail errors, and of Delay ($F_{[1,18]} = 42.655$, $p < .0001$, $\eta_p^2 = 0.703$), indicating that participants made proportionally more errors during the 7 days retrieval session. There was no significant Detail Type × Delay interaction ($F_{[1,18]} = 3.672$, $p = .071$, $\eta_p^2 = 0.169$; Figure 2f). Taken together, although there was a time-dependent increase in errors, and a higher incidence of errors in peripheral details, these errors were accounted for when calculating the corrected "Retrieval Success" score.

The above analyses were conducted for all successfully retrieved film clips. To confirm that the clips we classified as "vividly retrieved" at 0 day and at 7 days were retrieved with high detail, we also performed a sub-analysis including only those clips with story and vividness ratings of 3 or 4 following the in-scanner retrieval. A 2 × 2 repeated measures ANOVA was conducted with Detail Type and Delay for vividly retrieved clips as within-subject factors, and the number of correctly recalled details (Retrieval Success) as the dependent variable. The ANOVA revealed significant main effects of Detail Type ($F_{[1,18]} = 74.861$, $p < .0001$, $\eta_p^2 = 0.806$), with more peripheral details recalled than central elements, and of Delay ($F_{[1,18]} = 30.846$, $p < .0001$, $\eta_p^2 = 0.631$), indicating that participants recalled fewer details after 7 days. A significant Detail Type x Delay interaction ($F_{[1,18]} = 33.161$, $p < .0001$, $\eta_p^2 = 0.648$) showed that, even for "vividly retrieved" clips, memory for peripheral details declines more over time ($t_{[18]} = 6.291$, $p < .0001$) than memory for central elements ($t_{[18]} = 3.74$, $p = .001$) (Figure 2g).

For all successfully retrieved clips, we next correlated the vividness ratings (between 2 and 4) with the total number of reported details (combining central and peripheral detail scores) during the postscan retrieval sessions. We observed significant positive correlations between the vividness ratings and the number of reported details for all individual trials in the 0 day and the 7 days retrieval sessions (Pearson's correlation coefficient between vividness ratings and the total number of details for 0 day retrieval, $r = 0.388$, $p < .0001$;

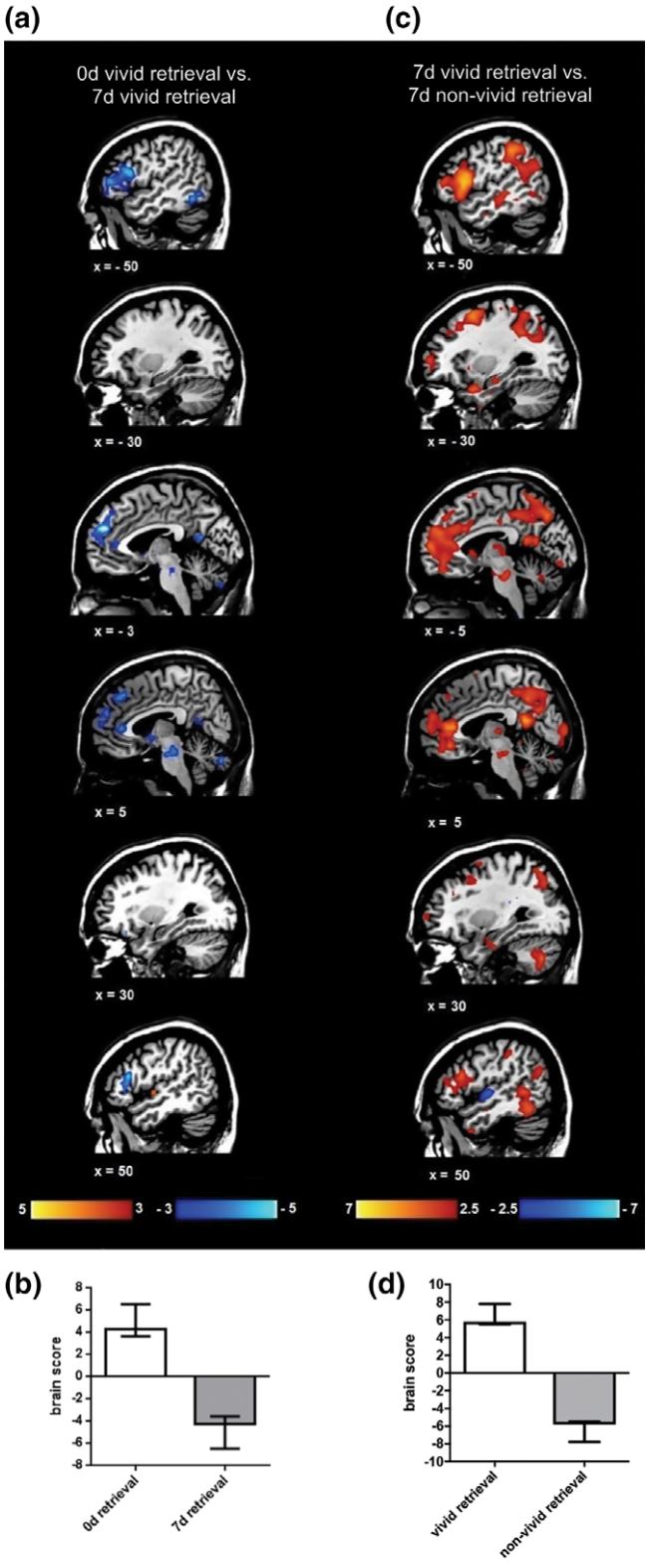

FIGURE 4 Vividly retrieved film clips do not differ in hippocampal activity during immediate and 7 days delayed retrieval. (a) LV depicting brain activity associated with immediate (0 d) vivid retrieval (warm colors) contrasted with 7 days (7 d) delayed vivid retrieval (cool colors). No differences were observed in hippocampal activation between the 0 and 7 days retrieval session. There is increased medial prefrontal activation, and pCC and angular gyrus activity accompanying memory vivid retrieval after 7 days. (b) Brain scores reflecting the degree to which 0 day vivid retrieval (positive BSRs) and 7 days vivid retrieval (negative BSRS) correlate with the pattern of activity seen in a. (c) LV depicting brain activity associated with 7 days vivid retrieval (warm colors) contrasted with 7 days nonvivid retrieval (cool colors). Note the bilateral hippocampal activity observed during vivid 7 days retrieval. (d) Brain scores reflecting the degree to which 7 days vivid retrieval (positive BSRs) and 7 days nonvivid retrieval (negative BSRs) correlate with the pattern of activity in c. Error bars are 95% confidence intervals [Color figure can be viewed at wileyonlinelibrary.com]

correlation coefficient between vividness ratings and the total number of details for 7 days retrieval, $r = 0.254$, $p < .0001$). See Figure 2h for plots of the vividness ratings and the number of retrieved details for successfully retrieved clips at each delay. Similar analyses conducted for vividness ratings and only peripheral details revealed a comparable pattern of results (data not shown, but available on request). These results confirm that the clips given high in-scanner ratings, and those classified as "vividly retrieved" were retrieved with high detail at each delay.

Analyses were also conducted to determine any gender differences in ratings and detailed memory retrieval using ANOVA with gender as a between-subject factor. We found a trending main effect of gender for ratings ($F_{[1,18]} = 4.072$, $p = .059$, $\eta_p^2 = 0.184$) with males rating the quality of their memory retrieval higher than did females, but no significant main effects or interactions for any other analyses (all $p > .1$).

4.2.2 | fMRI results: Analysis of BOLD activity

To test the prediction that recent, perceptually detailed memories for the film clips are supported by hippocampal activity, whereas older memories, being less perceptually detailed, yet retaining most central elements, are supported by medial prefrontal cortical regions, we assessed modulations of fMRI BOLD activity across the brain during film clip retrieval using Partial Least Squares (PLS). This multivariate approach to assessing co-varying patterns of activity is more sensitive than univariate approaches (Fletcher et al., 1996; Lukic, Wernick, & Strother, 2002), and allows us to take full advantage of fMRI's ability to identify brain-wide retrieval networks including and extending beyond the hippocampal and medial prefrontal cortical regions at each retrieval delay. To identify patterns of retrieval activity that characterized each delay, we first contrasted memory retrieval at each delay separately with a fixation control task. The significant increases in activity ($p < .001$) during immediate (0 d) retrieval are shown in warm colors in Figure 3a, and positive brain scores in Figure 3b. Immediate retrieval activated the middle and inferior temporal gyri, as well the medial temporal lobe, including the right parahippocampal cortex (cluster includes activity in the right anterior and posterior hippocampus), and the left fusiform gyrus (cluster includes activity in the left anterior and posterior hippocampus, and parahippocampal cortex). During immediate retrieval, activity also was evident in the prefrontal cortex, including clusters in the left inferior frontal gyrus and insular cortex, the right precentral gyrus, as well as the bilateral precuneus (See Table 1 [top] for full list of regions).

We next contrasted 7 days delayed retrieval with fixation. The significant activations above control activity ($p < .001$) seen at 7 days retrieval are shown in warm colors in Figure 3c, and positive brain scores in Figure 3d. Memory retrieval 7 days after encoding was

TABLE 3 Coordinates of regions associated with immediate and 7 days vivid retrieval

Hem	Brain region	BA	*X* (mm)	*Y* (mm)	*Z* (mm)	BSR	Cluster size (voxels)
0 day vivid retrieval > 7 days vivid retrieval							
Right	Insula lobe	13	48	−4	−4	4.98	10
0 day vivid retrieval < 7 days vivid retrieval							
Right	Anterior cingulate cortex[a]	32	16	36	20	−4.62	11
Right	Anterior cingulate cortex[a]	32	4	36	8	−5.35	26
Left	Superior middle frontal gyrus	9	−4	48	24	−6.2	129
Right	Middle frontal gyrus	47	40	48	0	−3.89	6
Right	Inferior frontal gyrus	45	56	24	8	−5.28	76
Right	Inferior frontal gyrus	47	32	28	−20	−4.73	13
Left	Inferior frontal gyrus	48	−56	20	16	−6.34	135
Left	Middle temporal gyrus	20	−56	−8	−24	−3.41	6
Right	Inferior temporal gyrus	37	48	−60	−16	−3.82	12
Left	Angular gyrus[a]	39	−48	−68	24	−3.51	7
Left	Posterior cingulate cortex[a]	17	−4	−60	16	−4.47	13
Right	Thalamus		12	−12	0	−4.53	20
Left	Thalamus		−8	−8	8	−3.48	7
Right	Cerebellum		12	−80	−32	−5.49	38
Right	Cerebellum	30	12	−44	−8	−4.92	6
Right	Cerebellum		28	−80	−32	−3.68	8
Left	Cerebellum		−4	−84	−40	−4.6	12
Right	Pons/brainstem		4	−24	−20	−4.77	31

Note. MNI coordinates of the peak activation voxel within each cluster are reported for LV1 for the PLS analysis of 0 day vivid retrieval (warm color activations in Figure 4a, positive BSRs) contrasted with 7 days vivid retrieval (cool color activations in Figure 4a, negative BSRs). Hem = hemisphere; BA = Brodmann Area; BSR = bootstrap ratio from the PLS analysis indicating the reliability of the reported voxel.
[a] Indicates the cluster contains structures within the retrieval network.

accompanied by activation in the left superior temporal gyrus and bilateral middle and inferior temporal gyri, as well as the medial temporal lobe, including the right anterior hippocampus and fusiform gyrus (cluster includes the right parahippocampal cortex), and the left fusiform gyrus (cluster includes the left hippocampus, and parahippocampal cortex). Distributed activity was also seen in the prefrontal cortex, including large clusters in the right superior frontal gyrus, bilateral middle and inferior frontal gyrus, bilateral insular cortex, as well as the right precuneus (See Table 1, bottom, for full list of regions).

To determine differences in the patterns of activity elicited during immediate and 7 days delayed memory retrieval, we directly contrasted retrieval-related activation at each delay. A significant pattern (p = .008) differentiating retrieval at the two delays showed more activity for immediate memory in the right posterior hippocampus and the bilateral precentral gyrus (Figure 3e warm colored regions, and positive brain scores in Figure 3f). Relative to 0 day, 7 days memory retrieval (Figure 3e cool colored regions, and negative brain scores in Figure 3f) activated the bilateral left middle frontal gyrus, inferior frontal gyrus and medial prefrontal cortex, including the bilateral superior medial frontal gyrus, as well as the right aCC (See Table 2 for full list of regions).

Together, these three PLS analyses identify retrieval-related activity in medial temporal and prefrontal cortical regions that is present across delays (when contrasted with fixation), and highlight a shift in the recruitment of these regions. Specifically, hippocampal and parahippocampal activity declines, but does not completely disappear, as activity in the medial and lateral prefrontal cortex increases over time. This shift in relative hippocampal and prefrontal activity as the memory ages and loses a disproportionate amount of peripheral detail mirrors the time-dependent pattern seen in rodents, where activity shifts toward the aCC as remote memory generalizes across contexts (Experiment 1).

To determine if retrieval of detailed episodic memory continues to elicit hippocampal activity in humans, we contrasted the immediate retrieval session and the 7 days delayed retrieval session only for clips that were rated as vividly retrieved (clips given in-scan perceptual vividness and story content ratings of 3 or 4). The in-scanner ratings, rather than the detail scores, were used to classify clips due to the fact that the ratings were a measure of performance taken immediately after each in-scanner retrieval trial. In this analysis, if older but vividly recalled memories continue to engage the hippocampus, we would not expect to see differences in hippocampal activity between these two conditions. As predicted, no delay-related differences in hippocampal or parahippocampal activity were found for vivid retrieval, although differences were evident in other brain regions. We identified a significant distributed pattern of activity (p = .017) that differentiated vivid memory retrieval between the two delays. This pattern indicated greater activity in a small cluster in the right insular cortex for immediate than for 7 days old vivid memory (Figure 4a warm colored regions, and positive brain scores in Figure 4b). Relative to 0 day, 7 days vivid memory retrieval (Figure 4a cool colored regions, and negative brain scores in Figure 4b) activated bilateral clusters in the inferior frontal gyrus and medial prefrontal cortex including the left superior medial frontal gyrus and the right aCC. Activity was also

observed in the pCC and angular gyrus (see Table 3 for full list of regions). This continued hippocampal activity, and distributed cortical activity observed after 7 days was accompanied by a slight reduction in the number of retrieved peripheral details (Figure 2g).

The absence of a significant difference in hippocampal activity between 0 and 7 days retrieval for vivid memories is consistent with the hypothesis that for vivid memories, the hippocampus is not differentially engaged at different delays. It should be noted, however, that the 7 days vivid retrieval analysis contains fewer trials than used in the previously reported analyses, and the failure to detect differences in hippocampal activation may, in part, be a result of low power. Therefore, to confirm the continuing role of the hippocampus during vivid memory retrieval after 7 days, we contrasted vivid retrieval with nonvivid retrieval during the 7 days session. The significantly greater activity ($p < .001$) seen during 7 days vivid retrieval is shown in warm colors in Figure 4c and positive brain scores in Figure 4d. Significantly greater activity during 7 days nonvivid retrieval is shown in cool colors, and negative brain scores. Vivid retrieval activated clusters in the medial temporal lobe, including bilateral hippocampus, and parahippocampal cortex. These results confirmed robust hippocampal activity during retrieval of highly vivid memories, but not for those equally aged memories retrieved with low vividness.

In line with the prediction that memories engage a changing network of brain regions over time, vivid retrieval of clips after 7 days, compared to nonvivid retrieval, was accompanied by additional activation of clusters in the medial and lateral frontal lobes, as well as in other regions typically involved in the retrieval network, including the middle temporal gyrus, bilateral pCC, precuneus, angular gyrus, and areas of the ventromedial prefrontal cortex. These results suggest a time-dependent broadening of the network supporting vivid memory retrieval that involves a shift toward increased recruitment of frontal nodes in the network (See Table 4 for full list of regions). Greater activity associated with 7 days nonvivid retrieval was found in small clusters in the right superior temporal gyrus and caudate.

5 | DISCUSSION

Using complementary neuroimaging approaches in rodents and humans, we show time-dependent changes in the quality of retrieved memories corresponding to changes in hippocampal-mPFC activity. Our results show that (a) the hippocampus is strongly activated during retrieval of context-specific memory in rats, and of detailed episodic memory in humans; (b) retrieval of general or schematic memory is supported by increased mPFC activity, and reduced hippocampal activity; (c) older memories that retain context-specificity (in rodents) or perceptual detail (in humans) continue to engage the hippocampus, yet increasingly recruit mPFC. These observations across species support the idea of a dynamic interplay between hippocampal and prefrontal cortical regions as memories transform over time, and suggest this interplay is influenced by both the age and the nature of the retrieved memory.

5.1 | The hippocampus continues to support context-specific and episodic memory

In rodents, the hippocampus was more active when memory was tested in the original conditioning context than in a novel context, regardless of the memory's age (Wiltgen et al., 2010). Optogenetic studies report that hippocampal neuronal ensembles engaged during memory acquisition continue to support context-specific memories. Although, over time, the network may distribute in the cortex, activation of the original cell assembly can induce expression of the context memory (Liu et al., 2012; Ramirez et al., 2013), while rapid inactivation leads to memory loss (Goshen et al., 2011). Likewise, in humans, 7 days vivid memory retrieval robustly engaged the hippocampus. The lack of difference in hippocampal activation between vivid retrieval at 0 and 7 days was likely not due to the limited clips that were vividly retrieved after 7 days, because retrieval of 7 days old vivid memories shows strong hippocampal activity when contrasted with nonvivid retrieval at that same timepoint.

Together, these findings support the notion that the *nature*, rather than the age, of a retrieved memory determines hippocampal recruitment in both species. If the memory remains detailed, vivid (humans) and context-specific (rodents), the hippocampus continues to support its representation (Winocur & Moscovitch, 2011) and does not disengage over time (Squire & Bayley, 2007).

5.2 | Medial prefrontal cortex activity increases as memories lose specificity

In rodents, mPFC becomes increasingly active during remote context memory retrieval (Frankland et al., 2004; Wheeler et al., 2013). Critically, we demonstrate that, unlike hippocampus, mPFC activity is relatively insensitive to the retrieval context. This finding helps resolve a long-standing debate concerning the nature of this representation. We suggest that a memory which becomes represented in mPFC is not an identical copy of the original memory, but rather a transformed, less detailed and vivid version that is qualitatively different from one which engages both regions (Winocur, Moscovitch, & Bontempi, 2010). Evidence from hippocampal lesion or inactivation studies supports this interpretation (Cullen, Gilman, Winiecki, Riccio, & Jasnow, 2015; Denny et al., 2014; Einarsson et al., 2014; Winocur et al., 2007). In agreement with Tonegawa, and colleagues, we find increasing involvement of the mPFC over time, even for information that still recruits the hippocampus strongly, consistent with the idea that mPFC engram cells develop over time (Tonegawa, Morrissey, & Kitamura, 2018; see also Sekeres et al, 2018).

Contrary to Tonegawa et al, we find no evidence, however, that context-specific memories in rodents, and perceptually detailed episodic memories in humans, are recovered without strong hippocampal involvement. Our results instead suggest that the mPFC is needed to retrieve schematic, context-general memories at long delays, and possibly also, that at such delays, these schematic memories serve as cues for retrieving detailed, context specific memories based on hippocampal representations.

In Experiment 2, the relative contributions of hippocampus and mPFC were mediated by the memory's age and qualitative content. Immediately following encoding, memories contained most of the

TABLE 4 Coordinates of regions associated with 7 days vivid and nonvivid retrieval

Hem	Brain region	BA	*X* (mm)	*Y* (mm)	*Z* (mm)	BSR	Cluster size (voxels)
7 days vivid retrieval > 7 days nonvivid retrieval							
Right	Superior frontal gyrus	8	20	20	60	−3.29	7
Right	Middle frontal gyrus	6	28	8	40	−3.56	35
Right	Middle frontal gyrus	6	28	4	64	−3.42	11
Right	Middle frontal gyrus	10	32	60	4	−3.71	13
Right	Inferior frontal gyrus	45	56	24	8	−4.56	113
Left	Inferior frontal gyrus	11	−20	40	−20	−5.16	6
Right	Anterior cingulate[a]	25	4	32	8	−5.59	239
Right	Anterior cingulate[a]	32	20	32	24	−3.86	5
Left	Precentral gyrus	48	−48	16	8	−6.89	866
Right	Parahippocampal gyrus[a]	36	32	−16	−32	−4.76	38
Left	Hippocampus[a]		−28	−20	−16	−4.72	14
Right	Parahippocampus[a]	20	40	−8	−20	−3.77	7
Right	Uncus	28	24	8	−24	−3.07	7
Right	Fusiform gyrus	37	44	−52	−12	−5.41	157
Left	Superior temporal gyrus	28	−24	8	−28	−5.29	48
Left	Superior temporal gyrus	22	−56	−48	20	−5.23	747
Right	Middle temporal gyrus	21	52	0	−24	−3.33	5
Left	Middle temporal gyrus	37	−56	−56	−4	−3.58	43
Left	Middle temporal gyrus	21	−56	−24	−16	−5.56	76
Left	Middle temporal gyrus	21	−68	−40	0	−3.23	6
Right	Suprmarginal gyrus	40	40	−40	36	−4.89	135
Left	Cingulate gyrus	23	−4	−8	32	−2.65	7
Right	Posterior cingulate[a]	30	4	−52	16	−5.9	239
Left	Posterior cingulate[a]	31	−12	−52	24	−2.97	6
Right	Precuneus[a]	7	36	−44	48	−3.02	7
Left	Postcentral gyrus	3	−40	−24	60	−3.21	11
Right	Lentifrom nucleus		24	0	−4	−3.59	7
Right	Lentifrom nucleus		16	8	−8	−3.16	8
Right	Caudate		20	4	8	−3.44	14
Left	Caudate		−8	12	0	−5.05	35
Right	Thalamus		12	−20	4	−5.28	139
Left	Pyramis		−8	−80	−40	−3.24	9
Right	Cerebellum		28	−68	−44	−4.94	194
7 days nonvivid retrieval > 7 days vivid retrieval							
Right	Caudate		24	−32	16	3.06	7
Right	Superior temporal gyrus	22	52	−12	0	4.59	26

Note. MNI coordinates of the peak activation voxel within each cluster are reported for LV1 for the PLS analysis of 7 days vivid retrieval (warm color activations in Figure 4c, positive BSRs) contrasted with 7 days nonvivid retrieval (cool color activations in Figure 4c, negative BSRs). Hem = hemisphere; BA = Brodmann Area; BSR = bootstrap ratio from the PLS analysis indicating the robust contribution of the reported voxel.
[a] Indicates the clusters falls within the retrieval network.

central elements defining the film's events, and peripheral (perceptual, contextual) details. Retrieval was supported by strong, bilateral activity in anterior and posterior hippocampus. After 7 days, many peripheral details were forgotten, while central elements were relatively preserved. Retrieval of this less-detailed, schematic memory was supported by increased activity in mPFC, and continued activation of anterior hippocampus. These findings are consistent with reports of functional specialization along the long-axis of the hippocampus, and its mPFC projections. Anterior hippocampus codes global representations related to the central elements of an event (Poppenk, Evensmoen, Moscovitch, & Nadel, 2013; Poppenk & Moscovitch, 2011; Robin & Moscovitch, 2017; Sekeres, Winocur, & Moscovitch, 2018). Accordingly, persistent activity in the anterior hippocampus during 7 days retrieval can account for both the increase in mPFC activity, and retrieval of the more schematic version of the memory (Ghosh, Moscovitch, Colella, & Gilboa, 2014). Reduced posterior hippocampal activity, and the decline of peripheral details and vividness after 7 days is consistent with the proposal that posterior hippocampus codes for finely detailed representations of an event (Moscovitch, Cabeza, Winocur, & Nadel, 2016).

Together, the results of both experiments are consistent with TTT, which proposes that a memory undergoes a transformation during which

its schematic features are represented cortically, whereas both fine and coarse contextual and perceptual details characterizing the original experience continue to be represented in the hippocampus (Moscovitch et al., 2016; Nadel & Moscovitch, 1997; Sekeres et al., 2018). To retrieve these details, the hippocampus remains necessary, regardless of the memory's age. Contextual cues prior to retrieval can reactivate the context-specific memory, and reinstate hippocampal dependency in rodents (Winocur et al., 2009) and humans (Cohn, Moscovitch, Lahat, & McAndrews, 2009), suggesting that both the generalized and detailed versions of memories can co-exist, with the conditions at the time of retrieval determining which version will be expressed.

A caveat to consider when using context fear conditioning to understand memory consolidation is the inclusion of aversive associative memories, which likely engages additional fear memory neural systems. However, earlier investigations report a similar shift toward mPFC activity as spatial memories age (Bontempi et al., 2000; Richards et al., 2014), suggesting a common transformation process operating on different types of hippocampal-dependent memories (Winocur et al., 2005, Winocur et al., 2009).

Loss-of-function studies have confirmed the necessity of the hippocampus in context-specific memories in rodents and perceptually-detailed episodic memories in humans (Winocur & Moscovitch, 2011). Correlational studies such as the present ones are important for understanding the recruitment of regions within the retrieval network under normal physiological conditions to better understand memory network dynamics. The present experiments tested for the continuing recruitment of the hippocampus over relatively short delays following memory encoding (7 days in humans, 30 days in rodents). While reduced hippocampal activity was observed as memories aged and lost detail, or generalized to other contexts, they did not completely disengage from the hippocampus, suggesting that, if intact, the hippocampus continues to participate in memory retrieval.

Given the current design, we cannot definitively state that the pattern of activity would be similarly observed after a period of months or years, although there is strong evidence for continuing hippocampal engagement during retrieval of decade old episodic memories (Bonnici & Maguire, 2017; Moscovitch et al, 2016). While the timeline for memory transformation is prolonged, changes in the BOLD response during retrieval of different aged memories may reflect the early stages of this process. One week may seem a short period of time to expect large-scale changes in networks supporting memory retrieval in humans, but reorganization of declarative memory networks has been detected just 24-hrs following memory acquisition (Ritchey, Montchal, Yonelinas, & Ranganath, 2015; Takashima et al., 2009). These findings suggest that reorganization of memory networks begins early, and may continue over the lifetime of a memory (Dudai, Karni, & Born, 2015).

5.3 | Reorganization of the memory network: Beyond hippocampus and mPFC

Investigation of whole-brain IEG activity following retrieval of recently acquired context memory in mice identified a network including hippocampus, medial temporal, and posterior parietal cortical regions (Vousden et al., 2015). These regions are similar to those we found active during recent memory retrieval in humans, suggesting that, despite noteworthy differences between animal and human memories, considerable overlap exists in the retrieval networks of both species. Chemogenetically silencing key hubs of the remote memory network in mice, including hippocampal CA1, reduced global efficiency of the network, and disrupted contextual fear memory (Vetere et al., 2017). This finding corresponds to similar deficits observed in humans after temporary inactivation of CA1 during transient global amnesia (Bartsch, Döhring, Rohr, Jansen, & Deuschl, 2011). How activity within the broader network in the rodent brain changes as a context-specific memory transforms over time remains unknown, but the results of Experiment 2 offer novel insight into this question.

In Experiment 2, immediate memory retrieval was supported by mPFC, hippocampus, parahippocampus, and posterior parietal activity. Not all regions of the retrieval network showed significant activity above the fixation control task, likely due to overlap with the default mode network (Spreng & Grady, 2010; Spreng, Mar, & Kim, 2009). Reduced activity throughout the posterior parts of this network (pCC, precuneus), was observed during 7 days retrieval. Given the involvement of these regions in recollection, this result suggests that recollective processes are not likely engaged during retrieval of detail-poor memories (McDermott, Szpunar, & Christ, 2009; Svoboda, McKinnon, & Levine, 2006). Other key regions of the retrieval network showed robust activity when memories were vividly (relative to nonvividly) retrieved after 7 days, including pCC and angular gyrus, areas typically associated with re-experiencing contextual and perceptual details during retrieval (Yonelinas, 2002). In turn, the shift toward prefrontal cortical activity within the network may reflect reliance on schematic knowledge (Ghosh & Gilboa, 2014; Gilboa & Marlatte, 2017), and the need for more attentional control and error monitoring (Cavanagh, Cohen, & Allen, 2009; Gilboa et al., 2006; Moscovitch & Winocur, 2002) during effortful retrieval of older memories.

Further investigations will determine the cellular mechanisms underlying memory transformation, how qualitative changes in memory are accompanied by shifts in functional connectivity between the hippocampus and mPFC, and changes in the weighting of key nodes in the retrieval network over time. Each of these avenues of research will require complementary contribution from studies of both humans and animals, with the ultimate goal of providing a neurobiological model of memory transformation across species.

ACKNOWLEDGMENTS

We gratefully acknowledge the technical assistance of Jeremy Audia, Christy Cole-Harding, Christa Dang, Nick Hoang, Daniel Nichol, Yao-Fang Tan, Annette Weekes-Holder, and Marilyne Ziegler. Additional financial support came from the Canada Research Chairs program, the Ontario Research Fund, the Canadian Foundation for Innovation, and the Heart and Stroke Foundation Centre for Stroke Recovery. We would also like to acknowledge the generosity of Jack Anne Weinbaum, Sam and Ida Ross, and Joseph Sandra Rotman in their support of the imaging centre at Baycrest. The human study was supported by CIHR grants to G.W. and M.M. (MOP125958), and to C.L. G. (MOP14036). The animal study was supported by an NSERC grant to G.W. (#A8181). M.J.S. was supported by a CIHR postdoctoral

fellowship. J.A.E.A. was supported by an NSERC Postgraduate Scholarship-Doctoral award and a Doctoral Completion Award from the University of Toronto.

CONFLICT OF INTEREST

The authors declare no competing financial interests.

AUTHOR CONTRIBUTIONS

Conceptualization: MJS, GW, MM, CLG; Methodology: MJS, GW, MM, JMW, MSL, MPM, CLG; Investigation: MJS, JAEA, SP; Writing—Original Draft: MJS, GW, MM, CLG; Writing—Review Editing: MJS, GW, MM, JAEA, SP, JMW, MSL, MPM, CLG; Funding Acquisition: GW, MM, CLG; Resources: JMW, MSL, GW, CLG; Supervision: GW, MM, CLG.

ORCID

Melanie J. Sekeres https://orcid.org/0000-0002-7952-3175

REFERENCES

Anagnostaras, S. G., Maren, S., & Fanselow, M. S. (1999). Temporally graded retrograde amnesia of contextual fear after hippocampal damage in rats: Within-subjects examination. *Journal of Neuroscience*, *19*, 1106–1114.

Anderson, J. A., Campbell, K. L., Amer, T., Grady, C. L., & Hasher, L. (2014). Timing is everything: Age differences in the cognitive control network are modulated by time of day. *Psychology and Aging*, *29*, 648–657.

Bartsch, T., Döhring, J., Rohr, A., Jansen, O., & Deuschl, G. (2011). CA1 neurons in the human hippocampus are critical for autobiographical memory, mental time travel, and autonoetic consciousness. *Proceedings of the National Academy of Sciences*, *108*(42), 17562–17567.

Ben-Yakov, A., & Dudai, Y. (2011). Constructing realistic engrams: Poststimulus activity of hippocampus and dorsal striatum predicts subsequent episodic memory. *Journal of Neuroscience*, *31*, 9032–9042.

Berntsen, D. (2002). Tunnel memories for autobiographical events: Central elements are remembered more frequently from shocking than from happy experiences. *Memory & Cognition*, *30*, 1010–1020.

Bird, C. M., Keidel, J. L., Ing, L. P., Horner, A. J., & Burgess, N. (2015). Consolidation of complex events via reinstatement in posterior cingulate cortex. *Journal of Neuroscience*, *35*, 14426–14434.

Bonasia, K., Sekeres, M. J., Gilboa, A., Grady, C. L., Winocur, G., & Moscovitch, M. (2018). Prior knowledge modulates the neural substrates of encoding and retrieving naturalistic events at short and long delays. *Neurobiology of Learning and Memory*. https://doi.org/10.1016/j.nlm.2018.02.017

Bonnici, H. M., Chadwick, M. J., Lutti, A., Hassabis, D., Weiskopf, N., & Maguire, E. A. (2012). Detecting representations of recent and remote autobiographical memories in vmPFC and hippocampus. *Journal of Neuroscience*, *32*, 16982–16991.

Bonnici, H. M., & Maguire, E. A. (2017). Two years later–revisiting autobiographical memory representations in vmPFC and hippocampus. *Neuropsychologia*, *110*, 159–169 [E-pub ahead of print].

Bontempi, B., Laurent-Demir, C., Destrade, C., & Jaffard, R. (1999). Time-dependent reorganization of brain circuitry underlying long-term memory storage. *Nature*, *400*(6745), 671.

Brainerd, C. J., & Reyna, V. F. (2002). Fuzzy-trace theory and false memory. *Current Directions in Psychological Science*, *11*, 164–169.

Campbell, K. L., Grigg, O., Saverino, C., Churchill, N., & Grady, C. L. (2013). Age differences in the intrinsic functional connectivity of default network subsystems. *Frontiers in Aging Neuroscience*, *5*, 73.

Cavanagh, J. F., Cohen, M. X., & Allen, J. J. (2009). Prelude to and resolution of an error: EEG phase synchrony reveals cognitive control dynamics during action monitoring. *Journal of Neuroscience*, *29*, 98–105.

Cohn, M., Moscovitch, M., Lahat, A., & McAndrews, M. P. (2009). Recollection versus strength as the primary determinant of hippocampal engagement at retrieval. *Proceedings of the National Academy of Sciences*, *106*(52), 22451–22455.

Cox, R. W. (1996). AFNI: Software for analysis and visualization of functional magnetic resonance neuroimages. *Computers and Biomedical Research*, *29*, 162–173.

Cullen, P. K., Gilman, T. L., Winiecki, P., Riccio, D. C., & Jasnow, A. M. (2015). Activity of the anterior cingulate cortex and ventral hippocampus underlie increases in contextual fear generalization. *Neurobiology of Learning & Memory*, *124*, 19–27.

Denny, C. A., Kheirbek, M. A., Alba, E. L., Tanaka, K. F., Brachman, R. A., Laughman, K. B., … Hen, R. (2014). Hippocampal memory traces are differentially modulated by experience, time, and adult neurogenesis. *Neuron*, *83*, 189–201.

Dudai, Y. (2012). The restless engram: consolidations never end. *Annual review of neuroscience*, *35*, 227–247.

Dudai, Y., Karni, A., & Born, J. (2015). The consolidation and transformation of memory. *Neuron*, *88*, 20–32.

Efron, B. (1981). Nonparametric estimates of standard error: The jackknife, the bootstrap and other methods. *Biometrika*, *68*, 589–599.

Einarsson, E. O., Pors, J., & Nader, K. (2014). Systems reconsolidation reveals a selective role for the anterior cingulate cortex in generalized contextual fear memory expression. *Neuropsychopharmacology*, *40*, 480–487.

Fletcher, P., Dolan, R., Shallice, T., Frith, C., Frackowiak, R., & Friston, K. (1996). Is multivariate analysis of PET data more revealing than the univariate approach? Evidence from a study of episodic memory retrieval. *NeuroImage*, *3*, 209–215.

Frankland, P. W., Bontempi, B., Talton, L. E., Kaczmarek, L., & Silva, A. J. (2004). The involvement of the anterior cingulate cortex in remote contextual fear memory. *Science*, *304*, 881–883.

Friston, K., Frith, C., Liddle, P., & Frackowiak, R. (1993). Functional connectivity: The principal-component analysis of large (PET) data sets. *Journal of Cerebral Blood Flow & Metabolism*, *13*, 5–14.

Furman, O., Mendelsohn, A., & Dudai, Y. (2012). The episodic engram transformed: Time reduces retrieval-related brain activity but correlates it with memory accuracy. *Learning & Memory*, *19*, 575–587.

Furman, O., Dorfman, N., Hasson, U., Davachi, L., & Dudai, Y. (2007). They saw a movie: Long-term memory for an extended audiovisual narrative. *Learning & Memory*, *14*, 457–467.

Garrett, D. D., Kovacevic, N., McIntosh, A. R., & Grady, C. L. (2010). Blood oxygen level-dependent signal variability is more than just noise. *Journal of Neuroscience*, *30*, 4914–4921.

Geib, B. R., Stanley, M. L., Wing, E. A., Laurienti, P. J., & Cabeza, R. (2015). Hippocampal contributions to the large-scale episodic memory network predict vivid visual memories. *Cerebral Cortex*, *27*(1), 680–693.

Ghosh, V. E., & Gilboa, A. (2014). What is a memory schema? A historical perspective on current neuroscience literature. *Neuropsychologia*, *53*, 104–114.

Ghosh, V. E., Moscovitch, M., Colella, B. M., & Gilboa, A. (2014). Schema representation in patients with ventromedial PFC lesions. *Journal of Neuroscience*, *34*, 12057–12070.

Gilboa, A., & Marlatte, H. (2017). Neurobiology of schemas and Schema-mediated memory. *Trends in Cognitive Sciences*, *21*, 618–631.

Gilboa, A., Alain, C., Stuss, D. T., Melo, B., Miller, S., & Moscovitch, M. (2006). Mechanisms of spontaneous confabulations: A strategic retrieval account. *Brain*, *129*, 1399–1414.

Goshen, I., Brodsky, M., Prakash, R., Wallace, J., Gradinaru, V., Ramakrishnan, C., & Deisseroth, K. (2011). Dynamics of retrieval strategies for remote memories. *Cell*, *147*, 678–689.

Grady, C. L., Protzner, A. B., Kovacevic, N., Strother, S. C., Afshin-Pour, B., Wojtowicz, M., … McIntosh, A. R. (2010). A multivariate analysis of age-related differences in default mode and task-positive networks across multiple cognitive domains. *Cerebral Cortex*, *20*, 1432–1447.

Greenberg, M. E., & Ziff, E. B. (1983). Stimulation of 3T3 cells induces transcription of the c-fos proto-oncogene. *Nature*, *311*, 433–438.

Kandel, E. R., Dudai, Y., & Mayford, M. R. (2014). The molecular and systems biology of memory. *Cell*, *157*(1), 163–186.

Kim, J. J., & Fanselow, M. S. (1992). Modality-specific retrograde amnesia of fear. *Science*, *256*, 675–677.

Liu, X., Ramirez, S., Pang, P. T., Puryear, C. B., Govindarajan, A., Deisseroth, K., & Tonegawa, S. (2012). Optogenetic stimulation of a hippocampal engram activates fear memory recall. *Nature*, *484*, 381–385.

Lukic, A. S., Wernick, M. N., & Strother, S. C. (2002). An evaluation of methods for detecting brain activations from functional neuroimages. *Artificial Intelligence in Medicine*, *25*, 69–88.

Mazziotta, J., Toga, A., Evans, A., Fox, P., Lancaster, J., Zilles, K., … Pike, B. (2001). A probabilistic atlas and reference system for the human brain: International consortium for brain mapping (ICBM). *Philosophical Transactions of the Royal Society of London B: Biological Sciences*, *356*, 1293–1322.

McDermott, K. B., Szpunar, K. K., & Christ, S. E. (2009). Laboratory-based and autobiographical retrieval tasks differ substantially in their neural substrates. *Neuropsychologia*, *47*, 2290–2298.

McIntosh, A., Chau, W., & Protzner, A. (2004). Spatiotemporal analysis of event-related fMRI data using partial least squares. *NeuroImage*, *23*, 764–775.

McIntosh, A., Bookstein, F., Haxby, J. V., & Grady, C. (1996). Spatial pattern analysis of functional brain images using partial least squares. *NeuroImage*, *3*, 143–157.

McIntosh, A. R., & Lobaugh, N. J. (2004). Partial least squares analysis of neuroimaging data: Applications and advances. *NeuroImage*, *23*(Suppl 1), S250–S263.

Moscovitch, M., & Winocur, G. (2002). *The frontal cortex and working with memory. Principles of frontal lobe function* (pp. 188–209). New York, NY: Oxford University Press.

Moscovitch, M., Cabeza, R., Winocur, G., & Nadel, L. (2016). Episodic memory and beyond: The Hippocampus and neocortex in transformation. *Annual Review of Psychology*, *67*, 105–134.

Nadel, L., & Moscovitch, M. (1997). Memory consolidation, retrograde amnesia and the hippocampal complex. *Current Opinion in Neurobiology*, *7*, 217–227.

Paxinos, G. W., & Watson, C. (1997). *The rat brain in stereotaxic coordinates*. Amsterdam, Netherlands: Elsevier Academic Press.

Poppenk, J., & Moscovitch, M. (2011). A hippocampal marker of recollection memory ability among healthy young adults: Contributions of posterior and anterior segments. *Neuron*, *72*, 931–937.

Poppenk, J., Evensmoen, H. R., Moscovitch, M., & Nadel, L. (2013). Long-axis specialization of the human hippocampus. *Trends in Cognitive Sciences*, *17*, 230–240.

Power, J. D., Barnes, K. A., Snyder, A. Z., Schlaggar, B. L., & Petersen, S. E. (2012). Spurious but systematic correlations in functional connectivity MRI networks arise from subject motion. *NeuroImage*, *59*, 2142–2154.

Ramirez, S., Liu, X., Lin, P.-A., Suh, J., Pignatelli, M., Redondo, R. L., … Tonegawa, S. (2013). Creating a false memory in the hippocampus. *Science*, *341*, 387–391.

Restivo, L., Vetere, G., Bontempi, B., & Ammassari-Teule, M. (2009). The formation of recent and remote memory is associated with time-dependent formation of dendritic spines in the hippocampus and anterior cingulate cortex. *Journal of Neuroscience*, *29*, 8206–8214.

Richards, B. A., Xia, F., Santoro, A., Husse, J., Woodin, M. A., Josselyn, S. A., & Frankland, P. W. (2014). Patterns across multiple memories are identified over time. *Nature Neuroscience*, *17*(7), 981–986.

Ritchey, M., Montchal, M. E., Yonelinas, A. P., & Ranganath, C. (2015). Delay-dependent contributions of medial temporal lobe regions to episodic memory retrieval. *eLife*, *4*, e05025.

Robin, J., & Moscovitch, M. (2017). Details, gist and schema: Hippocampal–neocortical interactions underlying recent and remote episodic and spatial memory. *Current Opinion in Behavioral Sciences*, *17*, 114–123.

Rugg, M. D., & Vilberg, K. L. (2013). Brain networks underlying episodic memory retrieval. *Current Opinion in Neurobiology*, *23*, 255–260.

Ryan, T. J., Roy, D. S., Pignatelli, M., Arons, A., & Tonegawa, S. (2015). Engram cells retain memory under retrograde amnesia. *Science*, *348*, 1007–1013.

Sampson, P. D., Streissguth, A. P., Barr, H. M., & Bookstein, F. L. (1989). Neurobehavioral effects of prenatal alcohol: Part II. Partial least squares analysis. *Neurotoxicology and Teratology*, *11*, 477–491.

Sekeres, M. J., Bonasia, K., St-Laurent, M., Pishdadian, S., Winocur, G., Grady, C., & Moscovitch, M. (2016). Recovering and preventing loss of detailed memory: Differential rates of forgetting for detail types in episodic memory. *Learning & Memory*, *23*, 72–82.

Sekeres, M. J., Moscovitch, M., & Winocur, G. (2017). Mechanisms of memory consolidation and transformation. In N. Axmacher & B. Rasch (Eds.), *Cognitive neuroscience of memory consolidation* (pp. 17–44). Cham, Switzerland: *Springer*.

Sekeres, M. J., Winocur, & Moscovitch, M. (2018). The hippocampus and related neocortical structures in memory transformation. *Neuroscience Letters*. doi:https://doi.org/10.1016/j.neulet.2018.05.006. [Epub ahead of print].

Spreng, R. N., & Grady, C. L. (2010). Patterns of brain activity supporting autobiographical memory, prospection, and theory of mind, and their relationship to the default mode network. *Journal of Cognitive Neuroscience*, *22*, 1112–1123.

Spreng, R. N., Mar, R. A., & Kim, A. S. (2009). The common neural basis of autobiographical memory, prospection, navigation, theory of mind, and the default mode: A quantitative meta-analysis. *Journal of Cognitive Neuroscience*, *21*, 489–510.

Squire, L. R., & Alvarez, P. (1995). Retrograde amnesia and memory consolidation: A neurobiological perspective. *Current Opinion in Neurobiology*, *5*, 169–177.

Squire, L. R., & Bayley, P. J. (2007). The neuroscience of remote memory. *Current Opinion in Neurobiology*, *17*, 185–196.

Squire, L. R., Genzel, L., Wixted, J. T., & Morris, R. G. (2015). Memory consolidation. *Cold Spring Harbour Perscpectives in Biology*, *7*(8), a021766.

St-Laurent, M., Moscovitch, M., & McAndrews, M. P. (2016). The retrieval of perceptual memory details depends on right hippocampal integrity and activation. *Cortex*, *84*, 15–33.

St-Laurent, M., Moscovitch, M., Jadd, R., & McAndrews, M. P. (2014). The perceptual richness of complex memory episodes is compromised by medial temporal lobe damage. *Hippocampus*, *24*, 560–576.

Svoboda, E., McKinnon, M. C., & Levine, B. (2006). The functional neuroanatomy of autobiographical memory: A meta-analysis. *Neuropsychologia*, *44*, 2189–2208.

Takashima, A., Nieuwenhuis, I. L., Jensen, O., Talamini, L. M., Rijpkema, M., & Fernández, G. (2009). Shift from hippocampal to neocortical centered retrieval network with consolidation. *Journal of Neuroscience*, *29*, 10087–10093.

Takashima, A., Petersson, K. M., Rutters, F., Tendolkar, I., Jensen, O., Zwarts, M., … Fernandez, G. (2006). Declarative memory consolidation in humans: A prospective functional magnetic resonance imaging study. *Proceedings of the National Academy of Sciences of the United States of America*, *103*, 756–761.

Tonegawa, S., Morrissey, M. D., & Kitamura, T. (2018). The role of engram cells in the systems consolidation of memory. *Nature Reviews Neuroscience*, *19*, 485–498.

Tulving, E. (1972). Episodic and semantic memory 1. In E. Tulving & W. Donaldson (Eds.), *Organization of London* (Vol. 381, pp. 382–404). New York, NY: Academic Press.

Vetere, G., Kenney, J. W., Tran, L. M., Xia, F., Steadman, P. E., Parkinson, J., … Frankland, P. W. (2017). Chemogenetic interrogation of a brain-wide fear memory network in mice. *Neuron*, *94*, 363–374 e4.

Vousden, D. A., Epp, J., Okuno, H., Nieman, B. J., van Eede, M., Dazai, J., … Lerch, J. P. (2015). Whole-brain mapping of behaviourally induced neural activation in mice. *Brain Structure and Function*, *220*, 2043–2057.

Wheeler, A. L., Teixeira, C. M., Wang, A. H., Xiong, X., Kovacevic, N., Lerch, J. P., … Frankland, P. W. (2013). Identification of a functional connectome for long-term fear memory in mice. *PLoS Computational Biology*, *9*, e1002853.

Wiltgen, B. J., & Silva, A. J. (2007). Memory for context becomes less specific with time. *Learning & Memory*, *14*, 313–317.

Wiltgen, B. J., Zhou, M., Cai, Y., Balaji, J., Karlsson, M. G., Parivash, S. N., … Silva, A. J. (2010). The hippocampus plays a selective role in the retrieval of detailed contextual memories. *Current Biology*, *20*, 1336–1344.

Winocur, G., & Moscovitch, M. (2011). Memory transformation and systems consolidation. *Journal of the International Neuropsychological Society*, *17*, 766–780.

Winocur, G., Moscovitch, M., Fogel, S., Rosenbaum, R. S., & Sekeres, M. (2005). Preserved spatial memory after hippocampal lesions: effects of extensive experience in a complex environment. *Nature Neuroscience*, *8*(3), 273.

Winocur, G., Moscovitch, M., & Sekeres, M. (2007). Memory consolidation or transformation: Context manipulation and hippocampal representations of memory. *Nature Neuroscience*, *10*, 555–557.

Winocur, G., Moscovitch, M., & Bontempi, B. (2010). Memory formation and long-term retention in humans and animals: Convergence towards a transformation account of hippocampal-neocortical interactions. *Neuropsychologia*, *48*, 2339–2356.

Winocur, G., Sekeres, M. J., Binns, M. A., & Moscovitch, M. (2013). Hippocampal lesions produce both nongraded and temporally graded retrograde amnesia in the same rat. *Hippocampus*, *23*, 330–341.

Winocur, G., Frankland, P. W., Sekeres, M., Fogel, S., & Moscovitch, M. (2009). Changes in context-specificity during memory reconsolidation: Selective effects of hippocampal lesions. *Learning & Memory*, *16*, 722–729.

Yonelinas, A. P. (2002). The nature of recollection and familiarity: A review of 30 years of research. *Journal of Memory and Language*, *46*, 441–517.

How to cite this article: Sekeres MJ, Winocur G, Moscovitch M, et al. Changes in patterns of neural activity underlie a time-dependent transformation of memory in rats and humans. *Hippocampus*. 2018;28:745–764. https://doi.org/10.1002/hipo.23009